國 立 交 通 大 學

工學院影像顯示科技產業研發碩士專班

碩 士 論 文

單、雙向延伸高分子分散液晶薄膜之研究

Uniaxial and Biaxial Extension Polymer Dispersed LC Films for Linear and Azimuthal Polarizers

研 究 生 ： 方彣綺

指導教授 ： 陳皇銘

中 華 民 國 九 十 七 年 六 月

單、雙向延伸高分子分散液晶薄膜之研究

Uniaxial and Biaxial Extension Polymer Dispersed LC Films for Linear and Azimuthal Polarizers

研 究 生：方 彣 綺　　Student : Wen-Chi Fang

指導教授：陳 皇 銘　　Advisor : Huang-Ming Philip Chen

國 立 交 通 大 學

工學院影像顯示科技產業研發碩士專班

碩 士 論 文

A Thesis

Submitted to

Industrial Technology R&D Master Program

on Imaging & Display

National Chiao-Tung University

for the Degree of

Master

In

Display Institute

June 2008

Hsinchu, Taiwan, Republic of China.

中 華 民 國 九 十 七 年 六 月

單、雙向延伸高分子分散液晶薄膜之研究

研究生：方彣綺　　指導教授：陳皇銘 博士

國立交通大學工學院影像顯示科技產業研發碩士專班

摘要

近 10 年來，平面顯示器蓬勃發展帶動了顯示器的革命，成功取代傳統 CRT 。在平面顯示器的熱潮中，由於液晶顯示器具有輕、薄的特性，並且各尺寸都有其應用產品，因此成為眾多平面顯示器中最重要的技術。能量的消耗對易於攜帶的液晶顯示器是很重要的考量因素，然而現階段應用於筆記型電腦的液晶平面顯示器其效能大約只有百分之六，最主要的能量損耗在於吸收式的偏極片。

研究顯示：拉伸過後的高分子分散液晶薄膜對光具有選擇性，藉由使用高分子分散液晶薄膜便可使散射的光在背光系統中回收再利用，使效能提升。本篇論文主要探討高分子分散液晶薄膜於拉伸過後的特性，並進一步將單向拉伸延伸至雙向拉伸，使其具有正方位極化的特性。

Uniaxial and Biaxial Extension Polymer Dispersed LC Films for Linear and Azimuthal Polarizers

Student: Wen-Chi Fang **Advisor: Dr. Huang-Ming Philip Chen**

Display Institute

National Chiao Tung University

Abstract

In the last one decade, flat panel displays have develop vigorously, promote the display revolution, and replace CRT successfully. In this current of flat panel displays, LCDs have the properties of light, thin, and have products of each size, so LCDs become the most important technology of numerous flat panel displays. For portable applications power consumption of a LCD is of the utmost importance. However, in typical high resolution LCDs utilized in laptop computer applications, the optical efficiency is approximately 6%. One of the primary reasons is the absorbing polarizers.

It has been reported that a stretched PDLC film has polarization selectivity. By utilizing these films for LCD applications, scattered light can be recycled in a backlight system to improve the optical efficiency. This thesis uses the PDLC material to fabricate stretched PDLC films and research the optical characteristics. Moreover, uniaxial extension is extended to biaxial extension to fabricate an azimuthal polarization converter.

誌謝

首先誠摯的感謝指導教授陳皇銘博士於兩年碩士班期間在實驗上與生活上的諄諄教誨、關懷與鼓勵。實驗上除了提供了良好的研究環境外，在實驗技巧上或概念想法上的努力指導，讓我對於液晶的特性有更深入的瞭解，也學習做事情該有的態度，在各方面都成長很多。另外感謝工業技術研究院提供的研究計畫，給予學生再研究上有更深一層的想法。

在兩年實驗室的生活，感謝淇文學長不吝指導與照顧，在研究上對我有莫大的幫助，特別感邱浩瑋同學，不論在實驗方向的協助與討論，以及幫助一些研究上所需要的量測，這些都辛苦你了。

我同時要離開校園的伙伴，文孚、蓮馨、謹瑋、怡帆、祥志，感謝你們在這段期間對於實驗上共同的努力、協助與生活上帶給我那歡樂的氣氛，這兩年實驗室共同的生活點滴是值得我一再回憶的。畢業後祝福同學們在未來人生道路上找到自己的目標和在各自的領域上有優異的成就。

接下來要感謝實驗室學弟智弋、宣穎、丞富及學妹毓筠，在有畢業壓力的碩二期間，有你們協助才能夠讓我在研究工作上能進行更順暢，也要感謝你們在負責儀器上與藥品採買上的付出，讓我們實驗室更上軌道。你們的加入也為實驗室增添了許多歡笑，讓兩年的研究生活變得更多采多姿。

最後我要感謝我的家人，感謝你們在求學的過程中不斷給予我鼓勵與支持，你們健康與快樂的生活是我能夠專注研究工作背後最大支柱，現在回憶這兩年生活，真的要感謝的人實在太多了，在此完成學業之際，僅以此獻給所有關心我及幫助我的人。

Table of Contents

List of Tables

List of Figures

Chapter 1

Introduction

1.1 Introduction of Liquid Crystal

Liquid crystalline phase is first discovered by Dr. F. Reinizer[1] in 1888 and the well known term "liquid crystal" is introduced by Lehmann[2] in 1890. In certain organic substances, composed of anisotropic molecules, the transition from the crystalline to the liquid state takes place in two or more distinct steps. In these materials between the solid and liquid states additional phases are formed which exhibit both liquid-like behavior and crystalline-like features. The substances showing this phenomenon are called liquid crystals, the intermediate phases are termed liquid-crystalline phase or mesophases.

The liquid crystal phases can be further divided into several various subphases, depending on the order of the molecular system. There are two main liquid crystal phases: the *nematic* phase which exhibits orientational order and no positional order, and the *smectic* phase which exhibits both orientational and partial positional order[3].

1.2 Liquid Crystal Phase

Liquid crystalline phases can be formed by many different types of molecules which differ widely in their structure. The typical LC molecular shapes are complicated, which can include the rod-like, discotic-like and the sanidic-like

shapes. In this thesis, the rod-like shape molecules are of main interest. The orientation of a rod-like molecule can be described by introducing two local axes, one parallel to the molecule known as long axis, and one perpendicular to it known as short axis. In general the molecules tend to align parallel to each other.

1.2.1 Nematic Phase

The nematic phase possesses an orientational order, but no positional order in a long range. In the nematic phase the molecular long axes are aligned, resulting in an averaged direction which is generally denoted with a unit vector **n** which is called director and represents the direction of the optic axis of the molecular system. The nematic phase is optically uniaxial due to the fact that although the molecular long axis is somewhat oriented, but all the directions perpendicular to the director are equivalent (figure 1.1).

On lowering the temperature of a nematic phase, additional orders such as positional order may appear. This can lead to a layered structure in the smectic phase and can be regarded as two dimensional liquids.

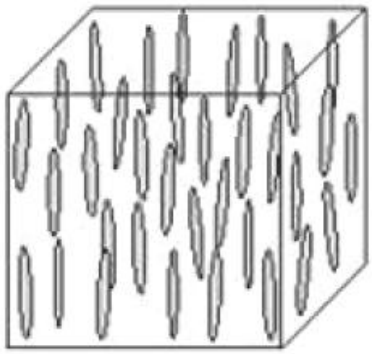

Figure 1.1 Nematic liquid crystals' alignment, the main axis is about point to the same orientation.

1.2.2 Smectic Phase

The smectic phase is close to the solid phase. Smectic liquid crystal molecules have one more degree of orientational order than nematic liquid crystal molecules. The molecules parallel to one another, forming a layer, but within the layer no periodic pattern exists. The liquid crystals are ordered in layers and normally float around freely inside these layers. The molecules tend to arrange themselves in the same direction. There are several different sub-phases to describe smectic phase. The two best known of these are smectic A and smectic C. In the smectic A phase, the molecules align perpendicular to the layer planes, and in the smectic C phase the alignment of the molecules is at some arbitrary angle to the normal (figure 1.2).

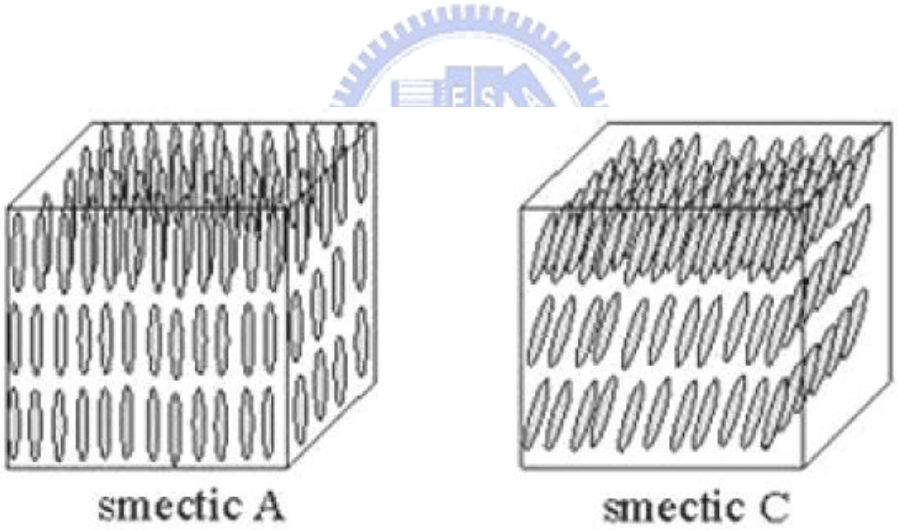

Fisure 1.2 Smectic liquid crystals are aligned in two dimensions and have layer structure.

1.2.3 Cholesteric Phase

The cholesteric liquid crystal phase is typically composed of nematic mesogenic molecules containing a chiral center which produces intermolecular forces that favor alignment between molecules at a slight angle to one another. Therefore,

two plane's long axis has an included angle. When the molecule's long axes in two adjacent planes have the same orientation, the distance between the two planes calls a pitch (fissure 1.3). From molecule's chirality we can decide the direction of rotation.

Cholesteric liquid crystals' pitch will change with different temperature, pressure, electric field, or magnetic field. Because this kind of liquid crystals has optical rotation, it can reflect the incident light with 2pn (n is average refractive index). Therefore, when the temperature is changed, it will happen to have a selective reflection because of different wavelengths and also causes a color variation. As a result, it can be used as a detector of temperature. Besides, the alignment of molecules are easily been effect by the electric field, it also can be reflective display, and electronic paper.

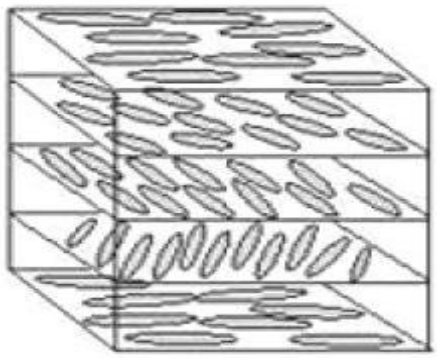

Figure 1.3 Cholesteric liquid crystals' helical structure, it can reflect the incident light.

1.2.4 Liquid Crystal Phases versus Temperature

The alignment of liquid crystal can be smectic phase or nematic phase, because the phase change can be related to temperature which is shown in figure 1.4.

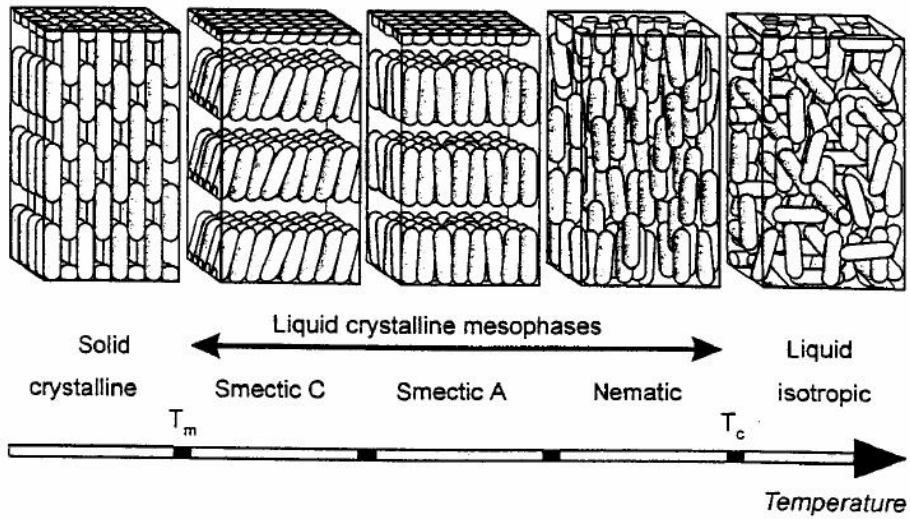

Figure 1.4 Schematic representation of molecular order between the crystalline, thermotropic LCs and liquid phase.

In nematic liquid crystals, it can be seemed as many small domains, each domain has molecules with the same orientation, different domain has different director. When light passes through, it causes scattering because of different director in the continuous domain. Therefore, the liquid crystals will be milky colored liquid. It only becomes transparent when all domains have the same orientation.

When the temperature is over T_{N-I}, the alignment of molecules will become isotropic and liquid state. It also makes the sample become transparent. This temperature calls clearing point and has significant physical meaning. Consequently, it's an important feature of liquid crystals that molecules will align orderly.

1.3 Polarizers of Liquid Crystal Displays Today[4,5,6]

Power consumption of a liquid crystal display (LCD) is of the utmost important for portable applications. In typical high resolution LCDs utilized in laptop computer applications, the optical efficiency is approximately 6%[7]. One of the primary reasons for the poor efficiency of an LCD is the presence of absorbing polarizers. Conventional polarizers based on absorption are iodide doped polyvinyl alcohol films that absorb >50% of the incident light (figure 1.5(a)).

In order to improve the optical throughput and efficiency of LCDs , a light recycling technique has been developed which uses nonabsorbing polarizers. The ideal concept of a nonabsorbing polarizer is one which efficiently reflects or backscatters light rather than absorbing it (figure 1.5(b) and (c)).

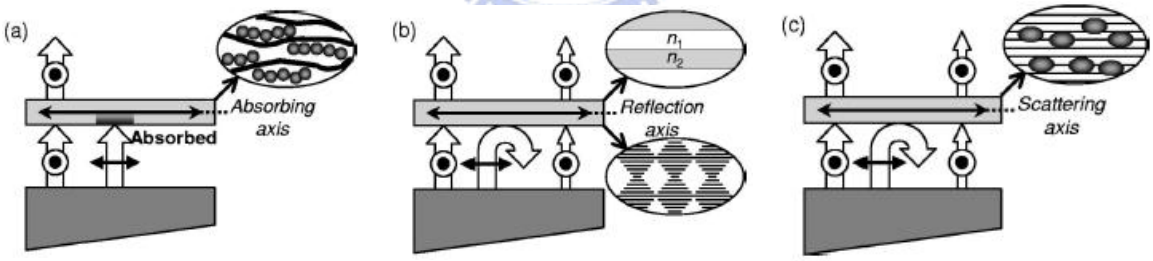

Figure 1.5 Configurations of various used in LCDs: absorbing (a), reflective (b), and light scattering (c).

It has been reported[8] that a stretched PDLC film has a polarization selectivity that arises from anisotropic scattering of aligned liquid crystal droplets in a polymer matrix as shown in figure 1.6. By utilizing these films for LCD applications, scattered light can be recycled in a backinght system to ultimately

improve the optical efficiency[9].

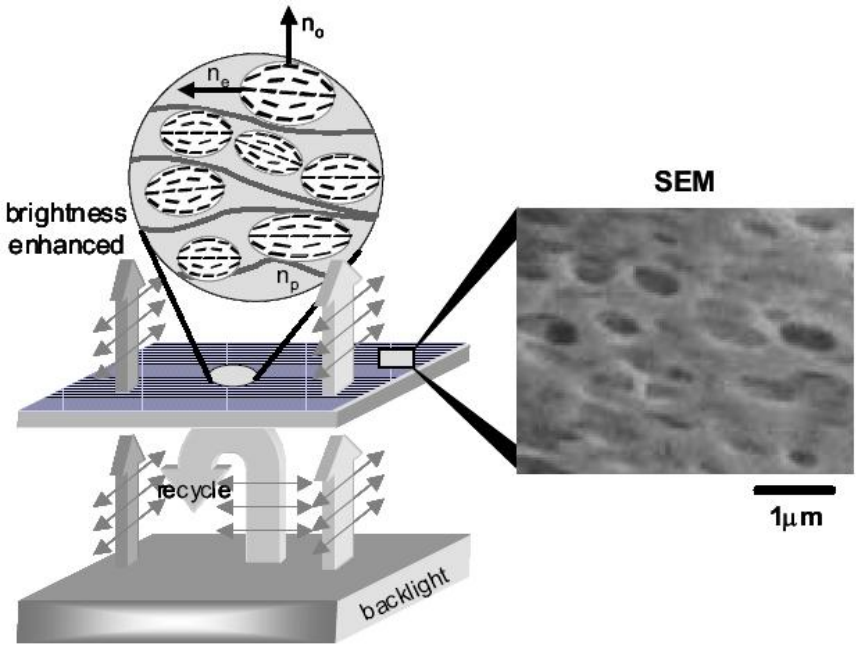

Figure 1.6 A scattering polarizer based on PDLC technology: the refractive index of polymer, n_p, matches that of the ordinary refractive index, n_o, of the liquid crystal.

1.4 Motivation and Objective

In conventional LCDs, the optical efficiency is approximately 6% because of absorbing polarizers. One of the ways to improve on the optical efficiency in an LCD is to replace these absorbing polarizers by reflective or scattering polarizers. Since scattering polarizers can possibly be less expensive to fabricate than reflective polarizers due to their simple structure and fabrication process and have the added benefit of recycling light that would have been absorbed in conventional polarizers. These devices can be viable candidates in protable LCDs where conserving power is one of the highest priorities.

A stretched PDLC film having a polarization selectivity which arises from

anisotropic scattering of aligned liquid crystal droplets in a polymer matrix can be applied to improve the optical efficiency of LCDs. As a result, the objective of this thesis is to fabricate stretched PDLC films and research the effects of light selectivity on the PDLC films. Moreover, uniaxial extension is extended to biaxial extension to fabricate to azimuthal polarizers[10,11]. Optical characteristics of the stretched PDLC films are also described in this thesis.

1.5 Organization of This Thesis

The rest of this thesis is organized as follows. The introduction and fabrication ways of polymer dispersed liquid crystal, and factors controlling alignment in LC droplets are presented in **Chapter 2**. In **Chapter 3**, the instruments used to measure the PDLC films will be described. The different fabrication ways of the PDLC films and the experiment results will be in **Chapter 4** and the extended experiment, “biaxial extension” will be in **Chapter 5.** The conclusion and future work of this thesis will be given in **Chapter 6**.

Chapter 2

Overview of Polymer Dispersed Liquid Crystals

2.1 Components of Polymer Dispersed Liquid Crystals[12]

Polymer dispersed liquid crystals (PDLCs) are a relatively new class of materials which was discovered until the early 1980's and hold promise for many application ranging from switchable windows to projection displays. These materials, which are simply a combined application of polymers and liquid crystals, are the focus of extensive research in the display industry. Other different types of polymer-liquid crystal composites with low concentration polymer networks that stabilize the bulk liquid crystal domains have been developed, such as polymer stabilized liquid crystal (PSLC), polymer network liquid crystal (PNLC), polymer stabilized cholesteric liquid crystal (PSCLC).

PDLCs have solid polymer matrix with liquid crystal droplets embedded in it. The LC droplets sizes (usually having bipolar configuration) range from hundred nano-meters to a few micro-meters. These tiny droplets are responsible for the unique behavior of the material. By changing the orientation of the liquid crystal molecules with an electric field[13], it is possible to vary the intensity of transmitted light.

PDLC windows are based on the ability of the nematic director of the piqued crystal droplets to align under an electric field. In a typical application, a thin

PDLC film (about 10 to 25 microns thick) is deposited between clear plastic covers. Transmission of light through a PDLC window depends primarily on scattering, which in turn depends on the difference in refractive index between droplets and their environment. In the case of high droplet density, the environment consists mainly of LC droplets, which makes the relative orientation of their directors an important factor. The droplets are anisotropic with the index of refraction parallel to the director different from that perpendicular to it. As sketched in figure 2.1, at voltage-off state, the random array of droplet orientation provides significant differences in indices and hence strong scattering. In this state, the cell appears opaque. On the contrary, light transparent the film at field-on state because the director of the individual droplets aligns with the field. There is now little difference in refrantive index for neighboring droplets, and the cell appears transparent.

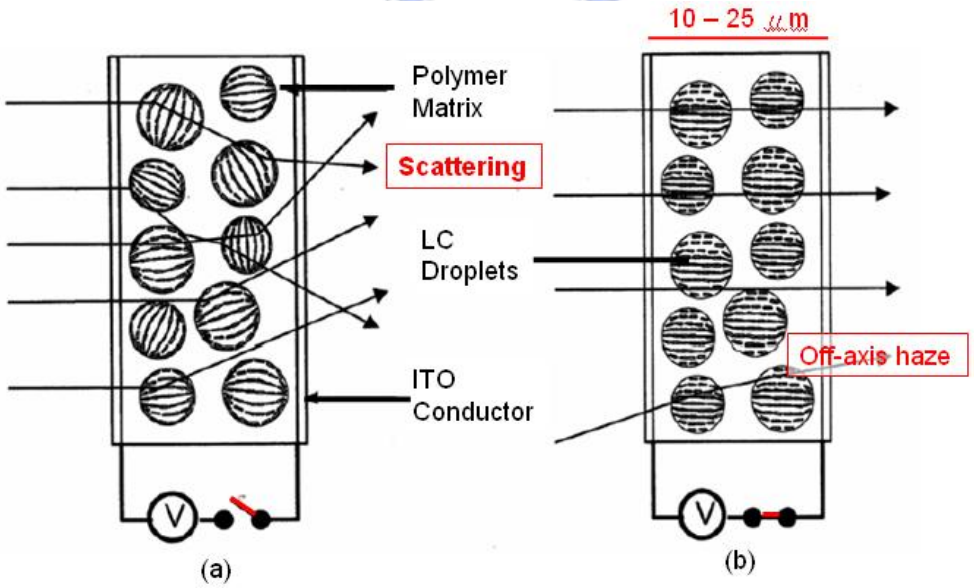

Figure 2.1 Operation principle of a PDLC shutter; (a) V=0; scattering state, (b) V≠0; transparent state.

2.2 Fabrication Ways of PDLCs

Polymer dispersed liquid crystals are usually produced in two distinct ways: encapsulation and phase separation[14,15]. Each method produces PDLCs with different properties and characteristics. Among the factors influencing the properties of the PDLC material are the size and morphology (shape) of the droplets, the types of polymer and liquid crystal used, and cooling and heating rates in production. The relationship between the method of production and these factors is explained below.

2.2.1 Encapsulation

Early attempts to produce PDLCs were made with a technique known as microencapsulation. In this method, a liquid crystal is mixed with a polymer dissolved in water. When the water is evaporated, the liquid crystal is surrounded by a layer of polymers. Thousands of these tiny “capsules” are produced and distributed through the bulk polymer. Droplets produced with this method tend to be non-uniform in size and can even be interconnected with each other. Materials fabricated by encapsulation are referred to as NCAP or nematic curvilinear aligned phase.

2.2.2 Phase Separation[16,17,18]

In order to obtain PDLCs by phase separation, a homogeneous mixture of polymer and liquid crystal is first produced. The liquid crystal droplets are then formed by the separation of the two phases. The separation can take place in one of the following three ways:

(1) Polymerization-Induced Phase Separation

Polymerization-induced phase separation (PIPS) occurs when a liquid crystal is mixed with a solution that has not yet undergone polymerization (a prepolymer). Once a homogeneous solution is formed, the polymerization reaction is initiated either thermally (thermoset polymer) or optically (photocurable polymer). Several PDLC sample have been obtained by an application of bias electric field intensity of 10-15 V/um and frequency of 150 Hz during curing the prepolymer. Because all used LC mixtures have positive anisotropy of dielectric permittivity, the longer droplets' axes have been aligned perpendicular to the glass plates. The principle of the method is shown in figure 2.2(a).

In addition, photopolymerization-induced phase separation (PPIPS) has been chosen as the most effective way to obtain ellipsoidal or flat LC droplets with extremely high aspect ration. The prepolymer can be cured by UV radiation. The curing rate, hence droplet size, has been adjusted by changing UV flux up to 20 W/cm^2. A slow unidirectional shearing of the upper glass plate with the respect of bottom one has been applied when the system has been partly cured up to the moment of full curing and PDLC stabilization. The scheme of the respective setup is given in figure 2.2(b).

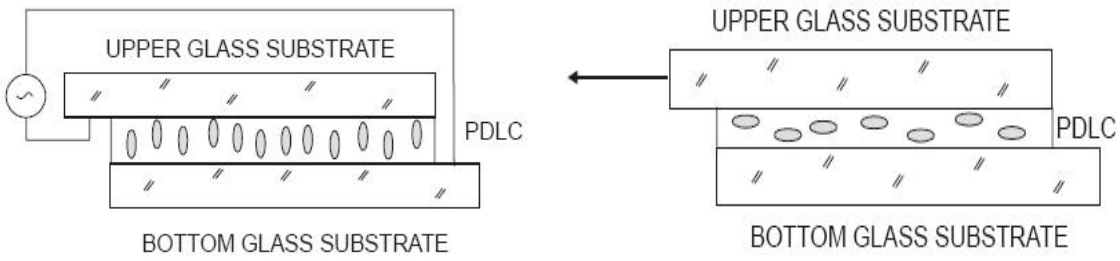

(a) (b)

Figure 2.2 Schematic presentation of the techniques used to elongate LC droplets in PDLC composite: (a) the deforming effect of electric field applied during PPIPS, (b) shearing of the system during PPIPS, an arrow represents the direction of the upper glass movement.

(2) Thermally-Induced Phase Separation

Thermally –induced phase separation (TIPS) can be used when the polymer binder has a melting temperature below its decomposition temperature. In this method, a homogeneous mixture of liquid crystal and a melted polymer is formed. The solution is cooled at a specific rate to induce phase separation. Liquid crystal droplets begin to form as the polymer hardens. The droplets continue to grow until the glass transition temperature of the polymer is crossed. Droplet size is affected the most by the cooling rate of the solution. Fast cooling rates tend to produce small droplets because there is not sufficient time for large particles to form. Therefore, droplet size and cooling rate are related inversely. Then the PDLC foil is carefully separated from the substrate , placed on heating rod and caught by clips one of which is steady while the second one is mounted on the movable stage driven by micrometric screw. In the heated region the elongation reached about 150 percent. Then the LC droplets elongated and flattened are stabilized by fast foil cooling. The scheme of the respective setup is given in figure 2.3.

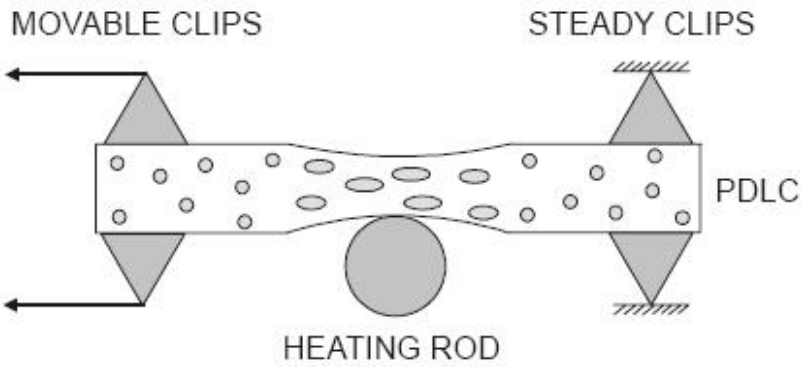

Figure 2.3 Schematic presentation of the techniques used to elongated LC droplets in PDLC composite: plastic stretching of the PDLC foil obtained by TIPS or SIPS.

(3) Solvent-Induced Phase Separation

The third common type of phase separation is called solvent-induced phased separation (SIPS). This process requires both the liquid crystal and polymer to be dissolved in a solvent. The solvent is then removed (typically by evaporation) at a controlled rate to begin the phase separation. Droplets start growing as the polymer and liquid crystal come out of solution and stop when all of the solvent has been removed. It still can be heated to elongate the LC droplets.

2.3 Factors Controlling Alignment in LC Droplets[19,20]

The configuration adopted by the (nematic) liquid crystal director field within a droplet reflects the subtle interplay of forces. The factors that determine the director configuration include the intrinsic, anchoring characteristics of the LCs, the presence of ecternal fields and the size (shape) of the droplets. The physical factors are:

Surface alignment

Surface alignment (between the liquid crystal and polymer binder) is the most important factor in determining the droplet configuration. Typically the anchoring energy which enforces this preferred alignment is quite strong compared to other elastic forces within the droplet. In the presence of strong surface anchoring force, the liquid crystals adopt a uniform tilt angle (either 0 or 90^{o}) at all points on the droplet surface.

Elastic constants

The balance of elastic forces within the droplet is the second important factor. To pack the liquid crystal into spherical shape, one or more defects were created. The elastic forces determine the structure within the droplet and the number (type) of defects. The relative values of the elastic constants K_{11}, K_{22} and K_{33} influence the preferred configuration of the director field within a cavity.

Droplet Size

The size of the cavity affects the elastic free energy density of the liquid crystals inside the droplets. In large droplets, the elastic forces (scale as curvature per unit length) are often too weak to force the LC directors. Many defects would exist to minimize the local free energy. The configurations in these droplets are complex.

Chapter 3

Measurement Systems

3.1 Overview of Measurement Systems

In this chapter, the measurement setups used in the experiments will be described in the following sections. The surface condition and the film thickness of PDLC films are observed by using α-step profilometer. Instrument such as polarizing optical microscope (POM), and laser optical system are utilized to characterize polarization and light selectivity. The size of LC droplets can be told by using the scanning electron microscope (SEM). The alignment of the LC droplets in polymer matrix can be observed by using Fourier transform infrared spectrometer (FT-IR). The major feature of the above mentioned instrument will be illustrated in this chapter.

3.2 α-Step Surface Profiler

α-Step surface profiler is a state-of –the –art, stylus-based surface profiler that combines high measurement precision with and economy. Ideal for applications such as semiconductor pilot lines and materials research, this advanced profiler enables faster process learning and higher yields. With guaranteed $8*10^{-10}$m (1 sigma) or 0.1% step height repeatability and sub-angstrom resolution, the α-Step provides excellent repeatability and performance to analyze and monitor processes. The diagram ofα-Step surface profiler is shown in figure 3.1.

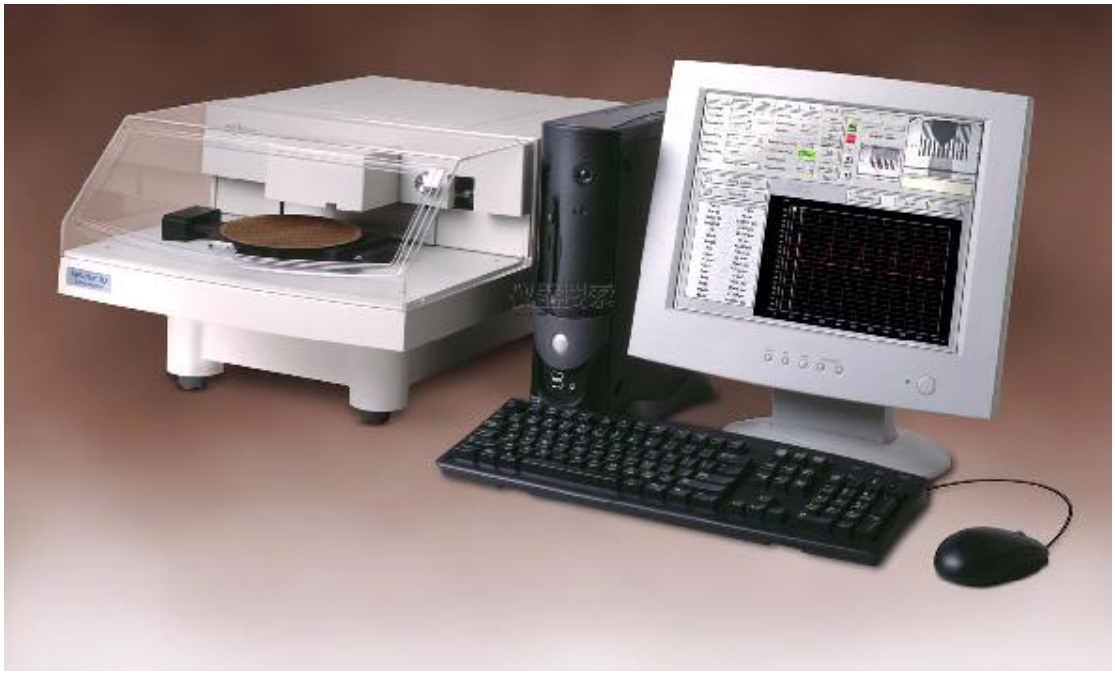

Figure 3.1 The picture of α-Step surface profiler.

3.3 Polarizing Optical Microscope (POM)

The polarized optical microscope is designed to observe and photograph specimens that are visible primarily due to their optically anisotropic character. In order to accomplish this task, the microscope must be equipped with both a polarizer, positioned in the light path somewhere before the specimen, and an analyzer (a second polarizer), placed in the optical pathway between the objective rear aperture and the observation tubes or camera port. Image contrast arises from the interaction of plane- polarized light with a birefringent specimen to produce two individual wave components that are each polarized in mutually perpendicular planes. Liquid crystal microphotographs were observed under POM, Olympus BX51 as shown in figure 3.2, the magnifications of POM are 100X, 200X, 500X and 1000X with changeable object lens of 10X, 20X, 50X and 100X, respectively, and a 10X eyepiece. Two measurable modes depend on transparent and reflective substrates are utilized with bottom light source and top

light source, respectively. An adjustable and movable polarizer can be utilized in both modes. Images observed under POM can be captured under CCD, and the parameter such as distance, area and angle can be calculated with its software.

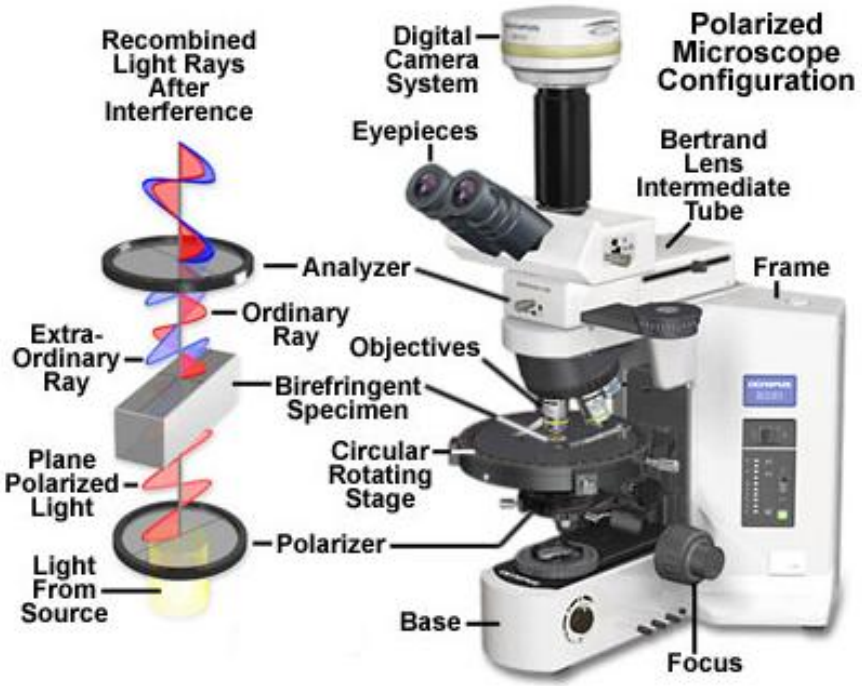

Figure 3.2 The concept and picture of POM Olympus BX51.

3.4 The Scanning Electron Microscope (SEM)

In light microscopy, a specimen is viewed through a series of lenses that magnify the visible-light image. However, the scanning electron microscope (SEM) does not actually view a true image of the specimen, but rather produces an electronic map of the specimen that is displayed on a cathode ray tube (CRT). The diagram of SEM is shown in figure 3.3. electrons from a filament in an electron gun are beamed at the specimen in a vacuum chamber. The beam forms a line that continuously sweeps across the specimen at high speed. This beam

irradiates the specimen which in turn produces a signal in the form of either x-ray fluorescence, secondary or backscattered electrons.

The SEM at GMU has a secondary electron detector. The signal produced by the secondary electrons is detected and sent to a CRT image. The scan rate for electron beam can be increased so that a virtual 3-D image of the specimen can be viewed. The image can also be captured by standard photography.

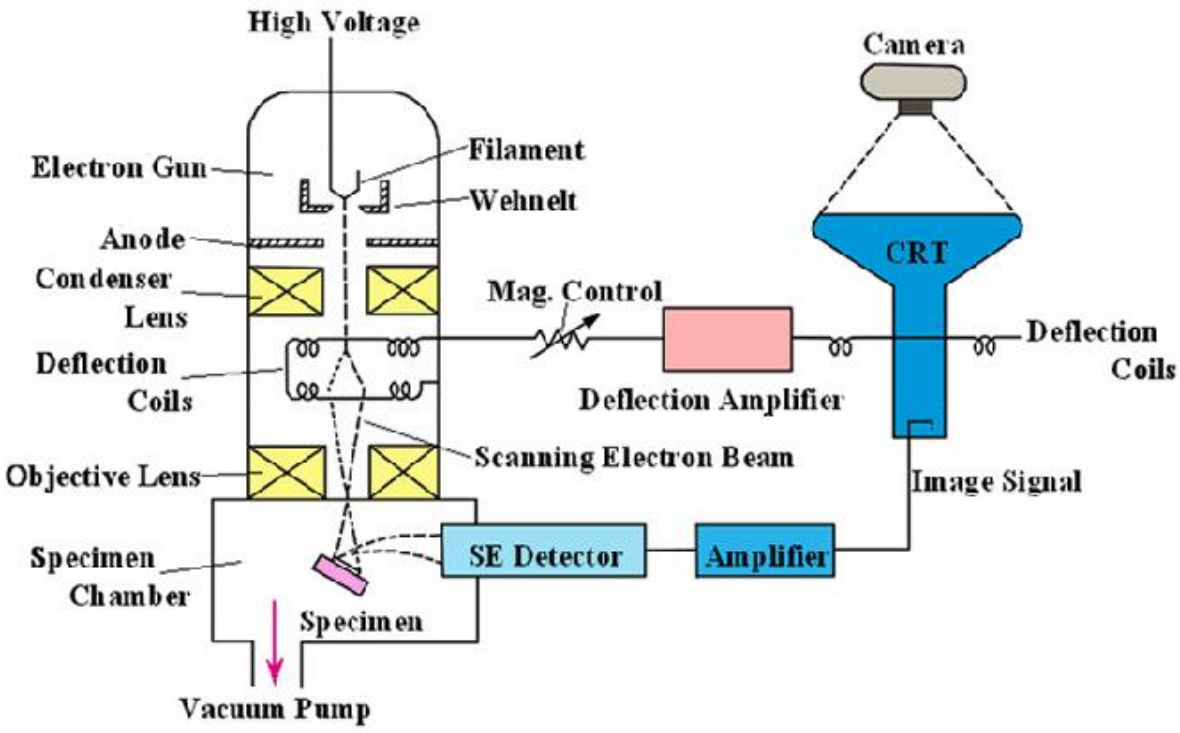

Figure 3.3 The diagram of the scanning electron microscope (SEM).

3.5 Fourier Transform Infrared Spectrometer (FT-IR)[21]

Fourier transform infrared (FT-IR) spectrometer has been extensively developed over the past decade and provides a number of advantages. Radiation containing all IR wavelengths (e.g., 4000-400cm^{-1}) is split into two beams. One beam is of fixed length, the other of variable length (movable mirror). The diagram of FT-IR is shown in figure 3.4 and 3.5.

The varying distances between two path lengths result in a sequence of constructive and destructive interferences and hence variations in intensities: an interferogram. Fourier transformation converts this interferogram from the time domain into one spectral point on the more familiar form of the frequency domain. Smooth and continuous variation of the length of the piston adjust the position of sample mirror and varies the length of the beam; Fourier transformation at successive points throughout this variation gives rise to the complete IR spectrum. Passage of this radiation through a sample subjects the compound to a broad band of energies. In principle the analysis of one broadband pass of radiation through the sample will give rise to complete IR spectrum.

There are a number of advantages to FT-IR methods. Since a monochromator is not used, the entire radiation range is passed through the sample simultaneously and much time is saved; FT-IR instruments can have very high resultion (<0.001cm^{-1}). Moreover since the data undergo analog-to-digital conversion, IR results are easily manipulated.

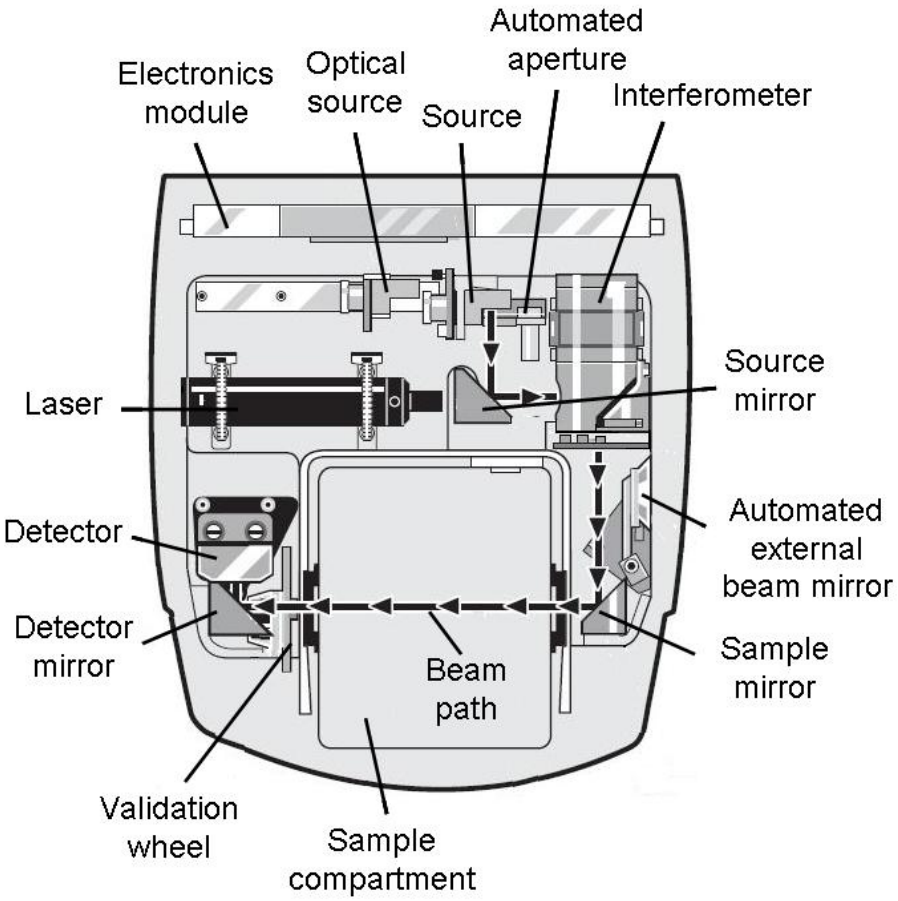

Figure 3.4 The scenograph of the FT-IR Spectrometer.

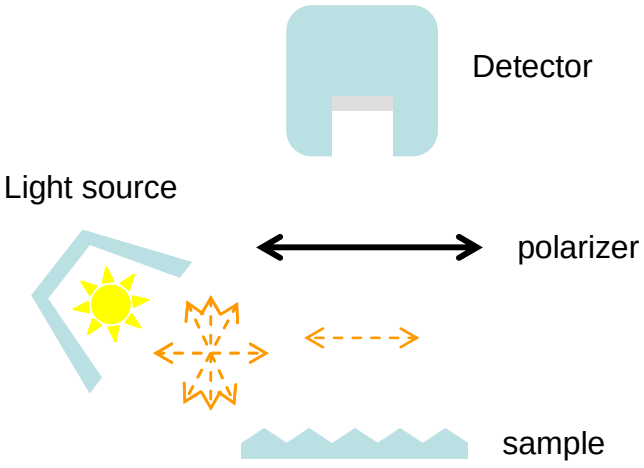

Figure 3.5 The diagram of the FT-IR Spectrometer.

Chapter 4

Results & Discussion of Uniaxial Extension

4.1 Methods to Obtain Deformed LC Droplets

Each method of PDLC preparation could be used to obtain composites nonspherical LC droplets, however, only phase separation techniques secure the proper control of droplets' size and shape. In this work we present four ways of preparation of elongated LC droplets in PDLC composites: R-to-R molding (by hand), spin coating, mold movement, and stretch and the results of each way will be described in this chapter..

4.2 Preparation of Elongated LC Droplets

General methods of PDLC preparation have been studied. In the case of encapsulation, the system is heterogeneous during the whole process. LC is dispersed in a polymer solution, the solvent of which does not dissolve LC. The solvent evaporation stabilizes the obtained composite structure due to polymer solidification.

4.2.1 Liquid crystal[22]

Nematic LC-E7 used as PDLC component has been prepared by Merck display technologies ltd.. It has been designed to meet standard PDLC requirements,

namely matching refractive indices of polymer and LC and fulfilling very low solubility of LC in cured polymer. The refraction indices of E7 are shown in table 4.1.

Table 4.1 Refraction indices of E7

n_e	n_0	Δn
1.745	1.52	0.225

4.2.2 R-to-R molding (by hand)

The way R-to-R molding is used to get shearing force to elongated LC droplets in PDLC composites. NOA65 is used as the polymer here. The properties of NOA65 are shown in table 4.2 and table 4.3 shows the refraction indices of E7 and NOA65.

Table 4.2 The properties of NOA65

materiality	materiality (25℃)	n_p	tensile ultimate
100%	1200cps	1.524	80%

modulus of elasticity (psi)	tensile strength (psi)	Hardness – shore D	temperature range (℃)
20000	1500	50	-15~60

Table 4.3 Refraction indices of E7 and NOA65

	n_o	n_e	Δn
E7	1.520	1.745	0.225
	n_p		
NOA65	1.524		

To prepare a PDLC cell, we mixed nematic LC E7 with an UV-curable monomer NOA65 at 25:75 wt%. We used an agitator to emulsify the liquid crystal into the NOA65 solution and used an ultrasonic probe to drive bubbles out. After the emulsion was prepared, it was coated on a mode with grooving and covered with a polyethylene terephtalate (PET) substrate using a rod. The film was cured by the UV-irradiation machine and peeled from the substrate. We tried three different pitches of modes for getting different shearing force, such as W=50um, 10um, and 4um, and D= 25um, 5um, and 2um..

We used a scanning electron microscope (SEM) and a polarizing optical microscope (POM) to observe the shape of LC droplets and the orientation. The observation of SEM and POM are sown in figure 4.1. and 4.2. According to these figures, the amounts of LC droplets are only a few, the size is about 1um and the orientation of LC droplets is not uniform.

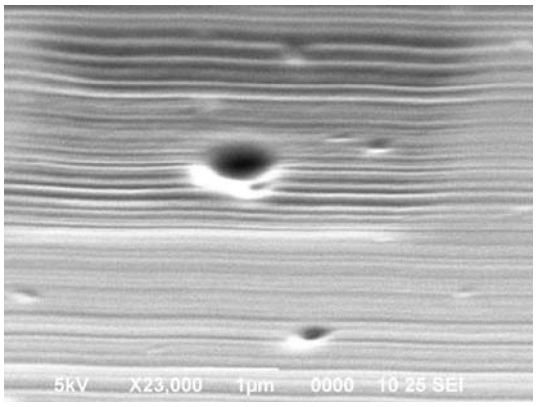

Figure 4.1 The SEM picture of E7/PVA PDLC film (magnification: 23000X)

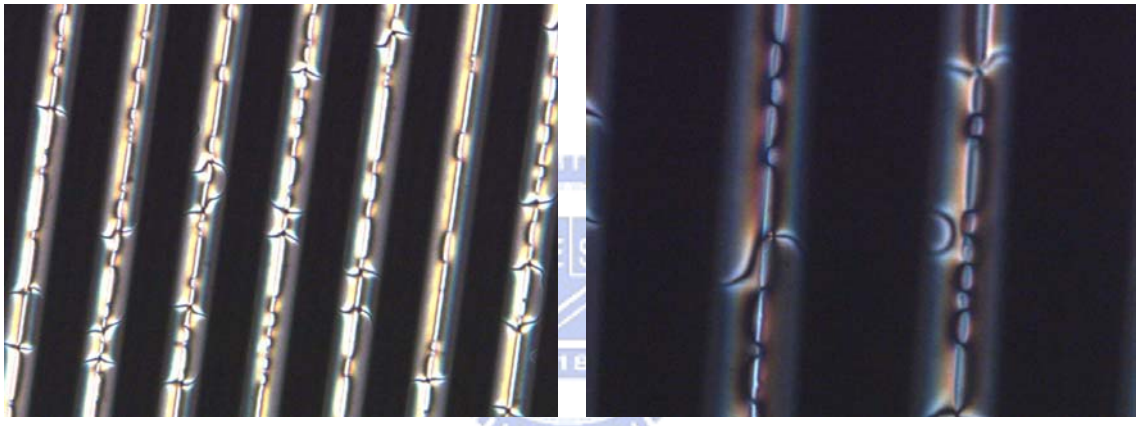

(a) (b)

Figure 4.2 The pictures of PDLC films made by R-to-R method taken by POM: magnification in (a) is 200X, in (b) is 500X.

In order to know the polarizing property of PDLC films, we used UV/Vis spectrophotometer- LAMBDA 950 and Fourier Transform Infrared Spectrometer (FT-IR) to observe. '-CN' is a representative functional-group of E7 and it absorbs a specific wave band at 2230cm^{-1}. We divided PDLC film into five parts shown in figure 4.3 and used FTIR to observe their absorption spectrums shown in figure 4.4.

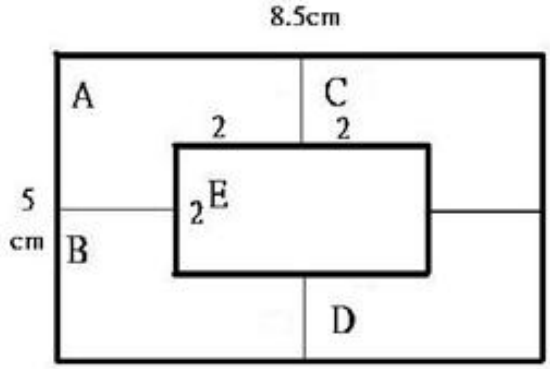

Figure 4.3 PDLC film is divided into five parts.

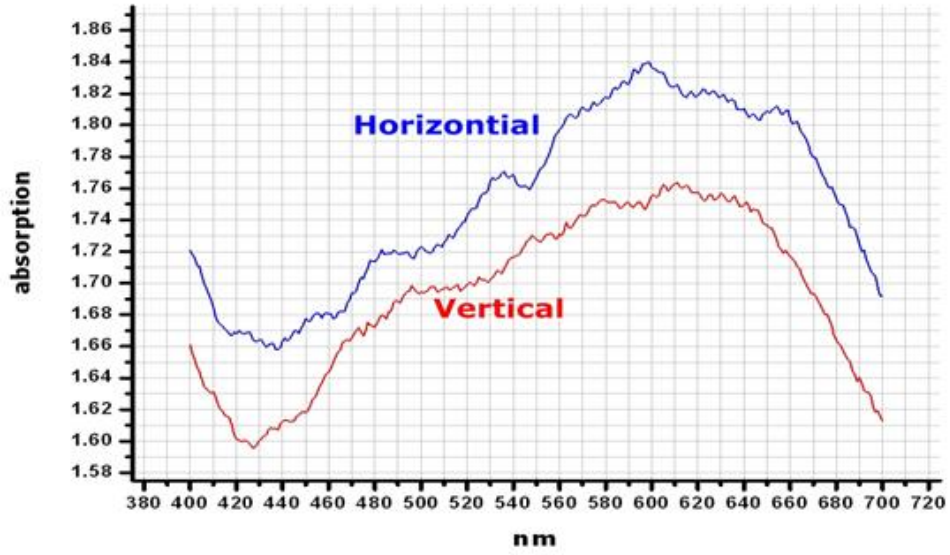

Figure 4.4 An absorption spectrum with light parallel (perpendicular) to the grooving of the film taken by UV/Vis spectrophotometer.

Use a formula as follow. We can get order parameters of each part.

$$\text{order parameter} = \frac{A_{//} - A_{\perp}}{A_{//} + 2A_{\perp}}$$

$A_{//(\perp)}$: absorption with polarization of light parallel (perpendicular) to the grooving of the film.

We found that each part of this film approximated to zero. It meant that LC droplets oriented almost randomly.

Figure 4.5(a) was taken by FT-IR with a tunable polarizer. The definitions of $A_{//}$ and $A_{\perp}$ are the same as that used in UV/Vis spectrophotometer. From figure 4.5(b) which is given by stacking two absorption spectrums in figure 4.5(a) at 2230cm^{-1}, polarization selectivity can be seen but not obviously.

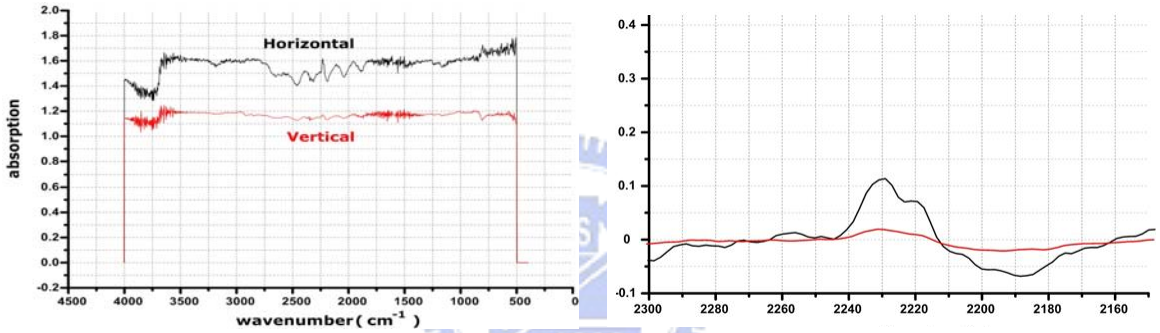

(a) (b)

Figure 4.5 (a): An absorption spectrum with light parallel (perpendicular) to the grooving of the film taken by FT-IR. (b): Stack up (a) at 2230cm^{-1}

According to the pictures taken by SEM and POM, and absorption spectrums taken by UV/Vis spectrophotometer and FT-IR, we can presume that the orientation of LC droplets in PDLC films made by R-to-R method is not uniform or LC droplets are not stretched during the process.

4.2.3 Spin Coating

The way-spin coating is used to get shearing force to elongated LC droplets in PDLC composites. NOA65 and E7 are the components of the PDLC films.

The preparation of LC/polymer solution is the same as which in R-to-R method. After the emulsion was prepared, it was coated on a PET substrate using a spin coater. During the process, we changed rotation rates to get different shearing force. The film was cured by the UV-irradiation machine.

In order to know the polarizing property of the PDLC film, we used spectrophotometer-LAMBDA 950 and FT-IR to check each part of films. The result is that we could not get effective polarizing property by spin coating method. The shearing force made by spin coating might not be influential enough to elongate and orient LC droplets.

4.2.4 Mold movement

The way-mold movement is used to get shearing force to elongated LC droplets in PDLC composites. NOA65 and E7 are the components of the PDLC films.

The preparation of LC/polymer solution is the same as which in R-to-R method. After the emulsion was prepared, put some emulsion on the substrate (PET) covered by the mold. A slow unidirectional shearing of the mold with respect to the substrate was applied. The film was cured by the UV-irradiation machine.

We used spectrophotometer-LAMBDA 950 and FT-IR to check each part of films. We still could not get effective polarizing property by way of mold movement. The reason we presume is that the elongated LC droplets recovered before cured and it's easy to get a lot of bubbles during mold movement.

4.2.5 Stretch

In this case, the way-stretch used to elongate LC droplets has been adopted. Commercial poly(vinyl chloride), chlorinated poly(vinyl chloride), poly(vinyl acetate) and poly(vinyl alcohol) have been chosen as polymer binder materials. Polyvinyl alcohol (PVA) is the polymer taken as PDLC component here. Table 4.4 shows the refraction indices of E7 and PVA.

The PDLC preparation process in case of polyvinyl alcohol (PVA) , which is a water-soluble polymer has been performed as fallows. At first a 20 wt% aqueous solution of PVA is mixed with the liquid crystal E7 and then dispersed in water. We used an ultrasonic probe to emulsify the liquid crystal into the PVA aqueous solution. The emulsion was coated on a smooth polyethylene terephthalate (PET) substrate using a Meyer Bar (figure 4.6) and dried in the sweatbox. The film was then peeled from the substrate. The film thickness was approximately 7-25um, which depends on the different Meyer Bars and humidity. The concentration of liquid crystal in the film is 25 wt%.

Table 4.4 Refraction indices of E7 and PVA

	n_o	n_e	Δn
E7	1.520	1.745	0.225
	n_p		
PVA	1.5		

The fabrication processes of PDLC polarizing films can be quantitatively understood by investigating the transmittance-strain behaviors associated with a

stretched PDLC. Testing begins with an unstretched PDLC film cut in the shape of a “dog-bone” sample shown in figure 4.7 connected to a load cell inside the tensile tester, with a Helium-Neon (He-Ne) laser operating at 633 nm probing the sample at normal incidence. Scattered light passing through the sample is filtered through an iris and was then on a power meter. The PDLC films were unidirectionally stretched by a tensile tester with the draw rate of 0.5 mm/min. A schematic representation of the optomechanical setup is shown in figure 4.8 and 4.9.

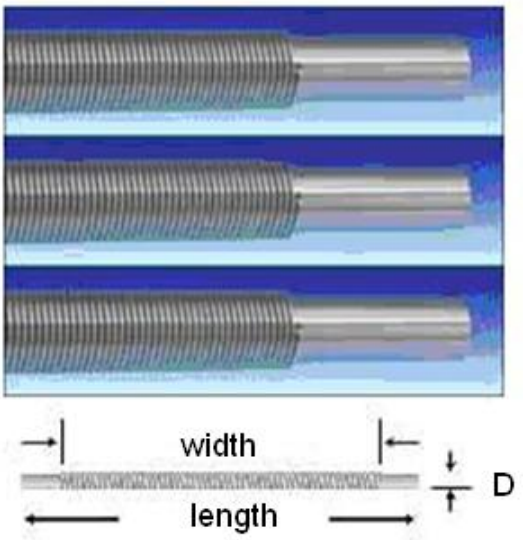

Figure 4.6 The picture of Meyer Bars.

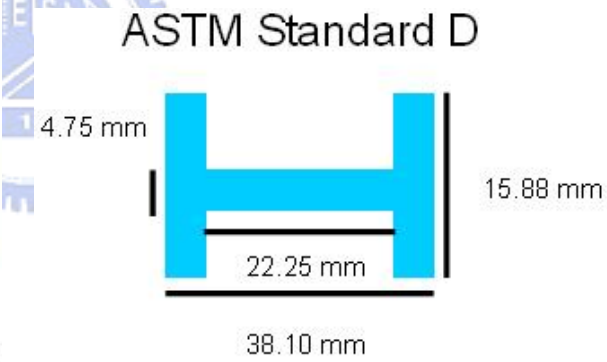

Figure 4.7 The standard of a “dog-bone” sample.

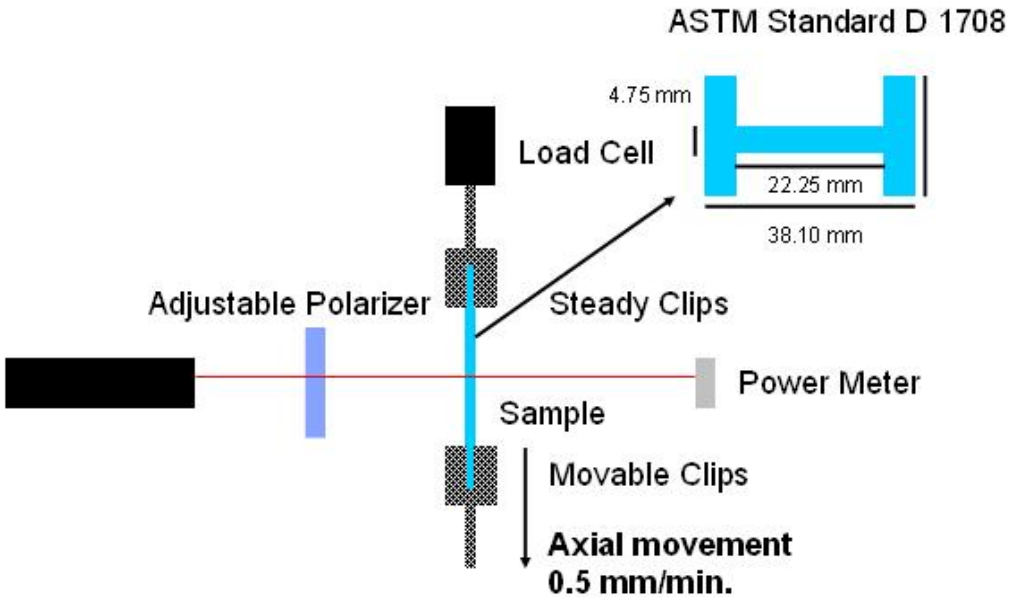

Figure 4.8 Schematic representation of optomechanical setup used for collecting measurements during applied strain.

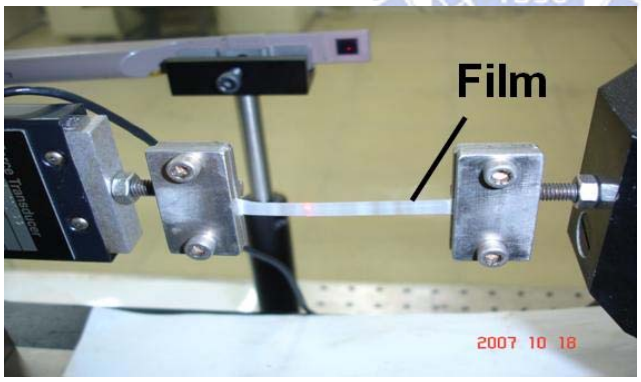

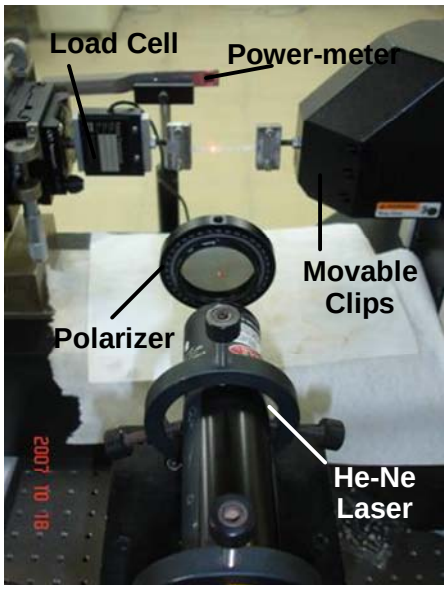

Figure 4.9 The pictures of the optomechanical setup.

4.2.5.1 Concentration Behavior of PDLC Films

We adjusted the concentration of liquid crystal (E7) in the film. The concentration was 20wt%, 25wt%, 35wt%, and 45wt%. After mixing well, repeat the experimental steps and compare the transmittance shown in figure 4.10.

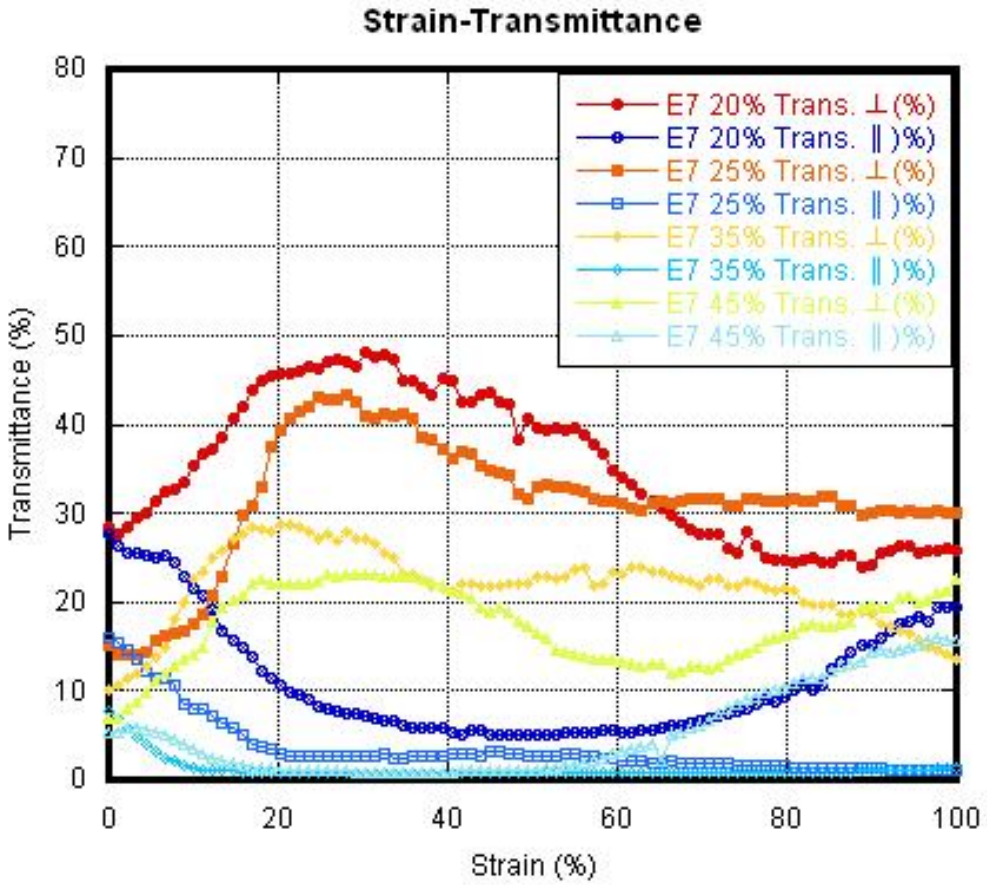

Figure 4.10 The strain-transmittance curve of the PDLC films with different concentrations of E7

From figure 4.10, we know that the transmittance is the highest at the concentration of E7 20wt%. Before stretching, the transmittance is approximately 30%. We can get the highest transmittance 50% when the strain

reaches 30%. Secondly, before stretching, the transmittance is about 18% at the concentration of E7 25wt% and it is 45% when the strain reaches 30%. From figure 4.10, we can see that the transmittance with polarization of light parallel and perpendicular to the tensile axis get closed when the strain reaches 50%. We could presume that defects occur at the surface of the film.

Next we compared the extinction ratios of each concentration to estimate its effect of polarization. The better the polarized property is the closer to zero the extinction ratio is. The formula of extinction ratio is as follow:

$$\text{Extinction Ratio} = T_{/\!/} / T_{\perp}$$

$T_{/\!/\ (\perp)}$: Transmittance with polarization of light is parallel (perpendicular) to the tensile axis of the film.

The extinction ratios of each concentration are shown in figure 4.11.

From figure 4.11, we can see that extinction ratios drop more rapidly as the concentration of E7 are 25wt%, 35wt% and 45wt% than it is 20wt% and the values are closer to zero. It means that we can get better effects of polarization at E7 25wt%, 35wt% and 45wt% than E7 20wt%.

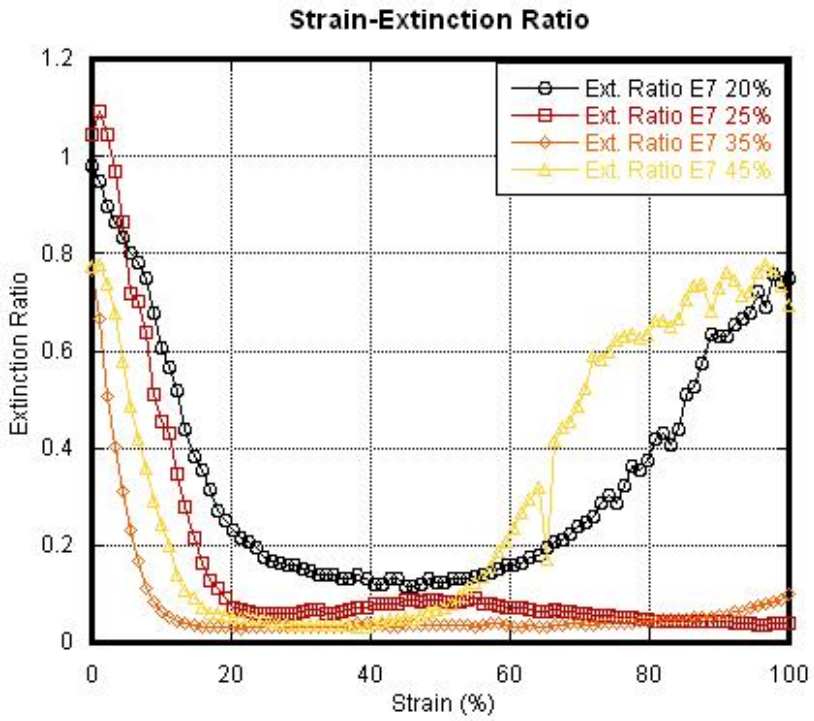

Figure 4.11 The extinction ratios of the PDLC films with different concentrations of E7

According to the transmittance and the extinction ratios, we choose E7 25wt% as the parameter of concentration.

4.2.5.2 Humidity Behavior of PDLC Films

As the concentration of E7 was 25wt%, we used the sweatbox to control the humidity. We dried the well coated PDLC films under humidity 20%, 30% and 40% respectively. After the films were dried and peeled from the substrate, they were stretched and measured the transmittance during the process. The diagrams of transmittance and extinction ratios versus strain are shown in figure 4.12 and 4.13.

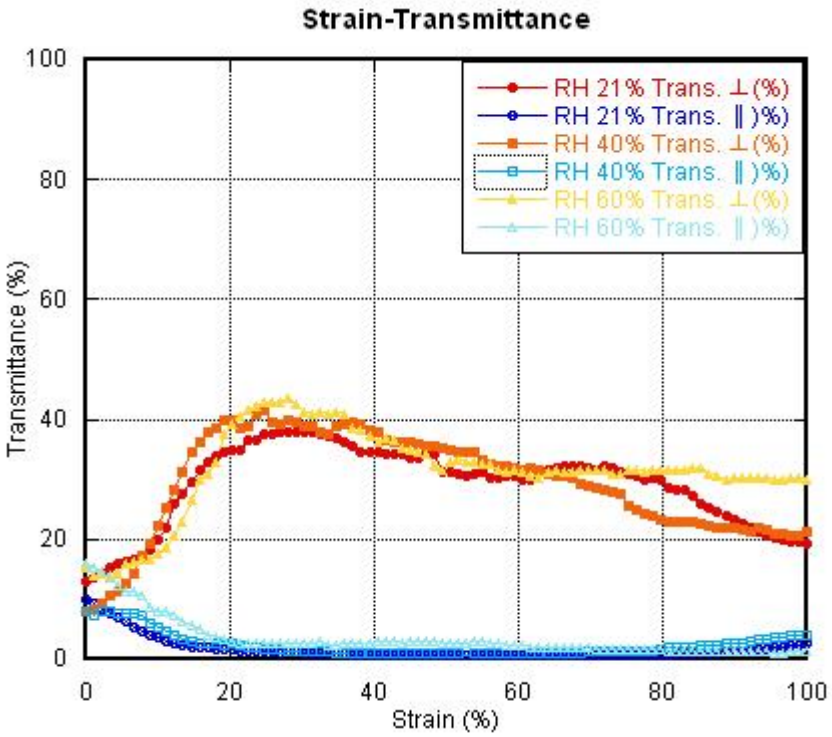

Figure 4.12 The strain-transmittance curve of the PDLC films with different humilities of drying condition.

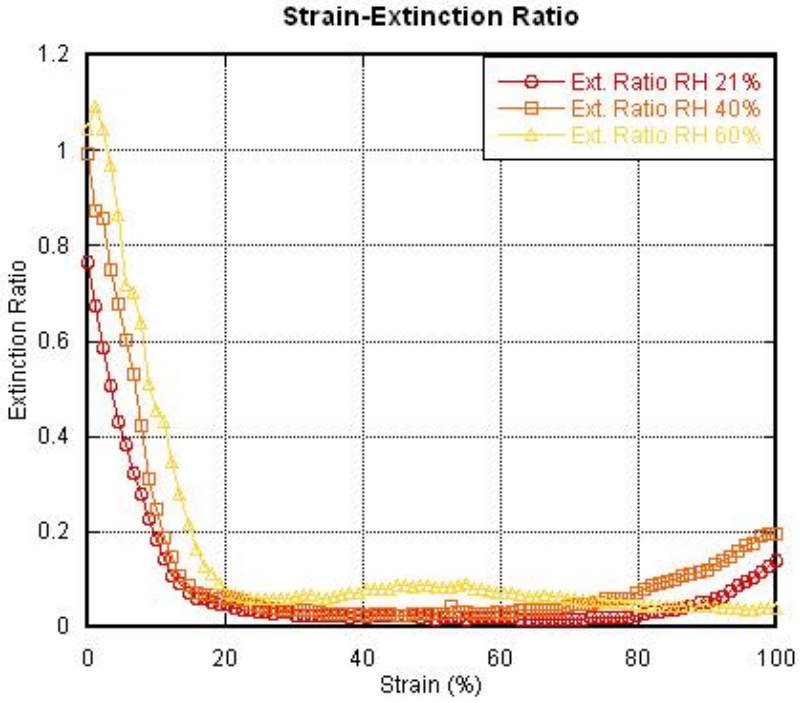

Figure 4.13 The extinction ratios of the PDLC films with different humilities of drying condition.

From figure 4.12 and 4.13, we could see that no matter what humidity the films were dried under, the tendency of transmittance and extinction ratios were similar and the values were almost equal. Therefore, it could be said that as long as the humidity was stable during the drying, the thickness of the films and the optical performance would be steady.

From now on, we choose 50% as the parameter of humidity because it is close to the laboratory conditions and easy to control.

4.2.5.3 Thickness Behavior of PDLC Films

As the concentration of E7 was 25wt%, and the humidity was 50%, we used Meyer Bars to get different thickness of PDLC films. There were three kinds of thickness about 10um, 15um and 20um. The films were cut in the shape of a 'dog-bone' sample, stretched and measured the transmittance during the process. The diagram of transmittance versus strain is shown in figure 4.14.

From figure 4.14, we could see that the transmittance of the thickness 11um (about 10um) is much higher than 14um (about 15um) and 20um, and it seemed to be that the thinner the film was, the higher the transmittance we could get. However, when the thickness of the film is thinner than 10um, the percentage of defects occurring at the surface of the film was about 50% when the strain reached 50%. This situation could be seen from figure 4.14 which the thickness of the films was about 10um. In this way, we didn't reduce the thickness to less than 10um since the transmittance would be higher. The extinction ratio versus strain is shown in figure 4.14.

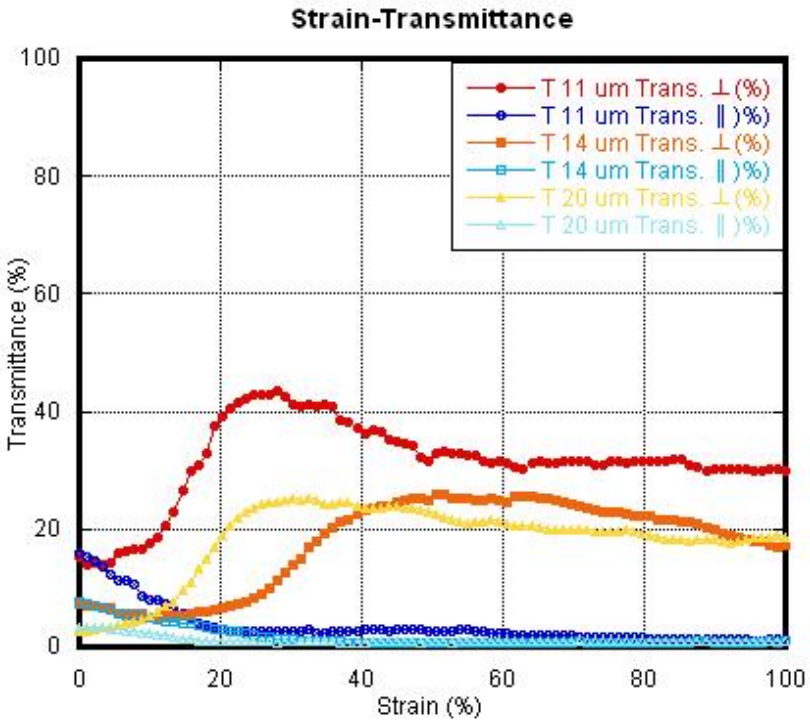

Figure 4.14 The strain-transmittance curve of the PDLC films with different thickness.

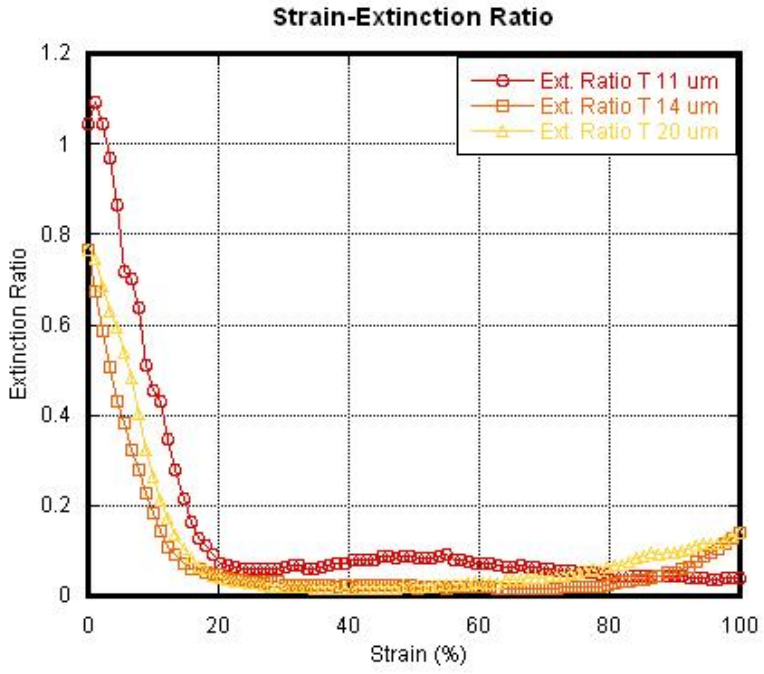

Figure 4.15 The extinction ratios of the PDLC films with different concentration of thickness.

From figure 4.15, we could see that the polarization effect of different thickness was no significant difference. In accordance with the transmittance, we take the films 10um as the parameter of the thickness in this experiment.

4.2.5.4 Polarizer Characteristic Experiment

As the concentration of E7 was 25wt%, the humidity was 50%, the thickness of the film was 10um, and it was cut in the shape of a “dog-bone” sample (standard specifications specimens D1708), we stretched the film till the strain was 30% and then fixed it like picture shown in figure 4.16. With a Helium-Neon (He-Ne) laser operating at 633 nm probing the sample at normal incidence, we rotated the polarizer to get a specifically polarized incident light. A schematic representation of photo shooting setup is shown in figure 4.17.

Figure 4.16 The picture of a “dog-bone” after being fixed.

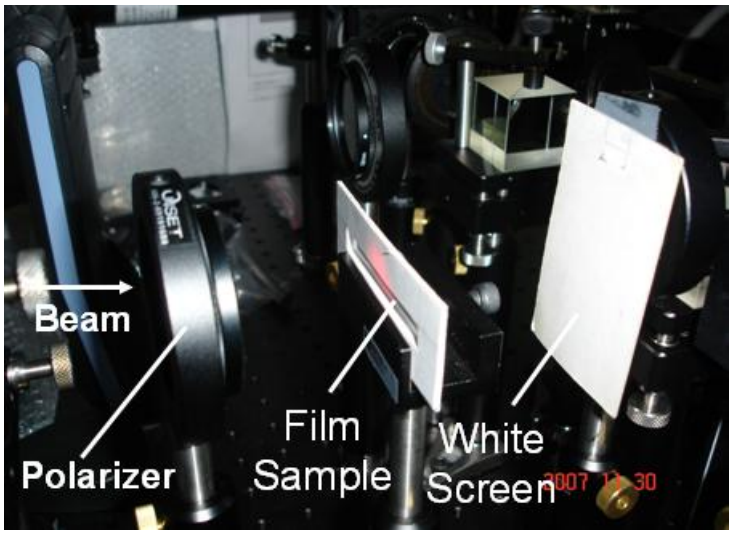

Figure 4.17 The picture of photo shooting setup

Figures of photo shooting are shown in figure 4.18. Figure 4.18(a) is that the polarization of the incident light is perpendicular to the tensile axis of the film. Figure 4.18(b) is that the polarization of the incident light is parallel to the tensile axis. Comparing figure 4.18(a) and (b), the stretched PDLC film really has a polarization selectivity.

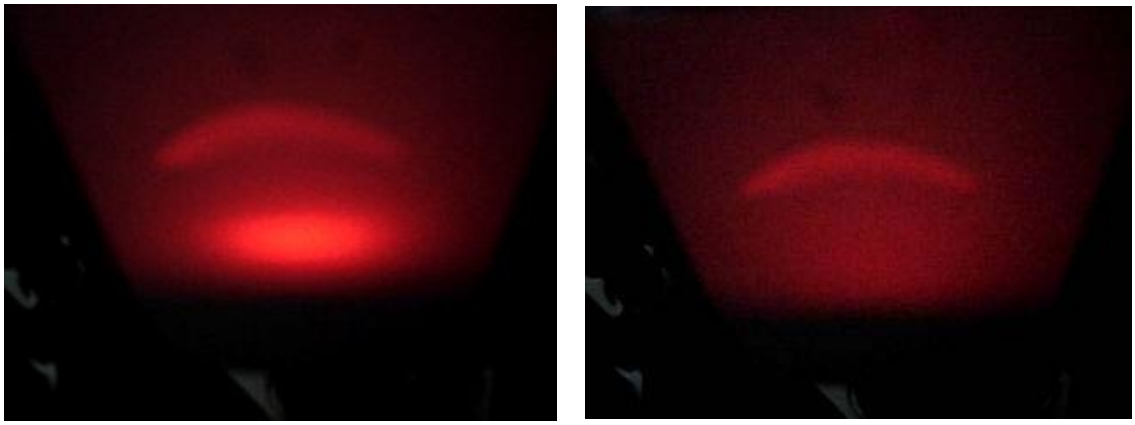

(a) (b)

Figure 4.18 (a): The picture is taken while the polarization of the incident light is perpendicular to the tensile axis. (b): The picture is taken while the polarization of the incident light is parallel to the tensile axis.

4.2.5.5 Transmittance vs. Scattering

From the result of the polarizer characteristic experiment, the stretched PDLC film has the property of linear polarizer. To be a scattering polarizer, we care about each percentage of transmittance and scattering. Therefore, the conoscopic detector (without polarizer) is used to measure each percentage of transmittance and scattering. Figures of conoscopic detector are shown in figure 4.19 and 4.20. Figure 4.19 is taken while the LED transmits the PDLC film whose thickness is 10um. Figure 4.20 is taken as the scattering of the PDLC film. A mirror is applied to be ATR.

Each percentage of transmittance and scattering measured from the different thicknesses of the PDLC films are shown in table 4.5. From table 4.5, we can see that the transmittance of the PDLC films is about 30% while the percentage of the scattering is about 35%.

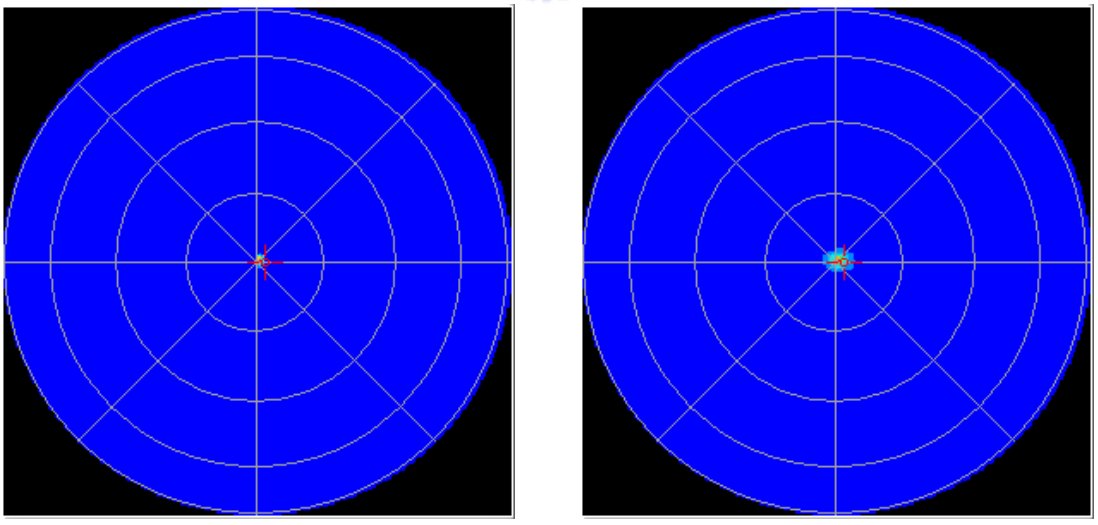

(a) (b)

Figure 4.19 The figure of the transmittance taken by conoscopic detentor (a) without sample while (b) with PDLC film.

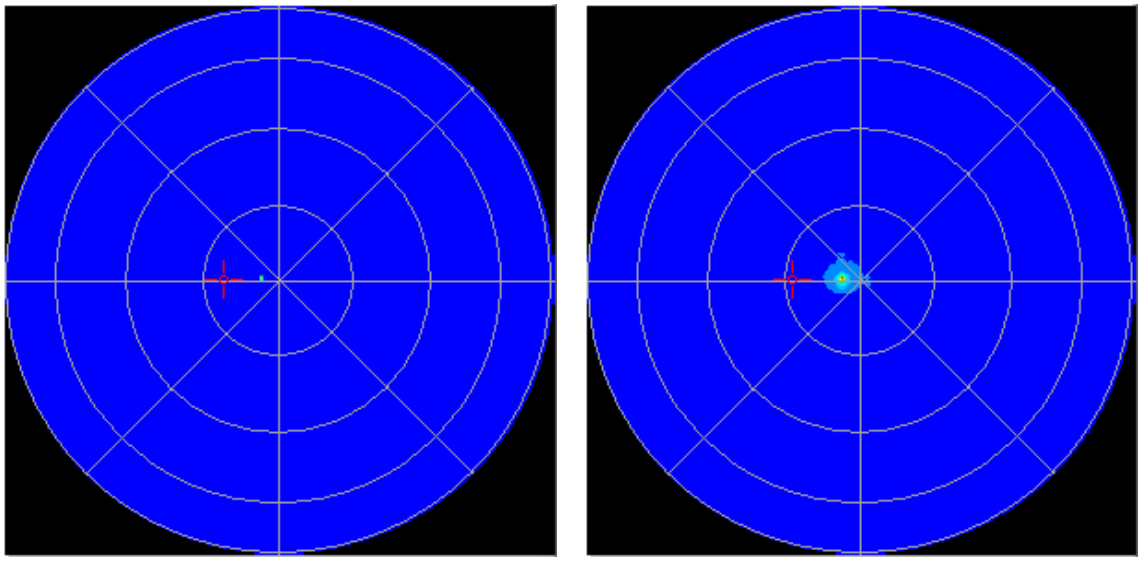

(a) (b)

Figure 4.20 The figure of scattering taken by conoscopic detentor (a) with a mirror as ATR while (b) with PDLC film.

Table 4.5 Transmittance vs. Scattering

	10um	15um	20um
Transmittance	29.60%	27.64%	24.28%
Scattering	35.22%	34.07%	37.06%

4.3 Companions of proposed methods

Table 4.6 Companions of proposed methods

Process	Material	Substrate	Success or Failure	Reason
R-to-R Molding (by hands)	E7 25wt% NOA65 75wt%	PET	Failure	Before curing, the elongated LC recover
Spin Coating	E7 25wt% NOA65 75wt%	PET	Failure	Before curing, the elongated LC recover
Mold Movement	E7 25wt% NOA65 75wt%	PET	Failure	Before curing, the elongated LC recover / Bubbles within film
Stretch	E7 25wt% PVA 75wt%	-- (PET)	Available	--

Chapter 5

Results & Discussion of Biaxial Extension

5.1 Biaxial Extension of PDLC Films

In former section, we discuss about linearly polarized. Now with the same way-stretch, we want to confer about optical characteristics of azimuthally polarized.

First, we prepared PDLC films. We took polyvinyl alcohol (PVA) as polymer and E7 as liquid crystals. According to the parameters setting in former section, the concentration of E7 was 25wt%, and the humidity was 50%.

Because biaxial extension was used in azimuthally polarized different from uniaxial extension in linearly polarized, the parameter of thickness here should be regulated. PDLC film was cut in the shape of a round sample whose radius was 16mm, fixed by the film holder, and stretched by the tensile tester with the draw rate of 0.5 mm/min. The setup is shown in figure 5.1. In figure 5.1, O-ring was used to prevent the film from broken easily.

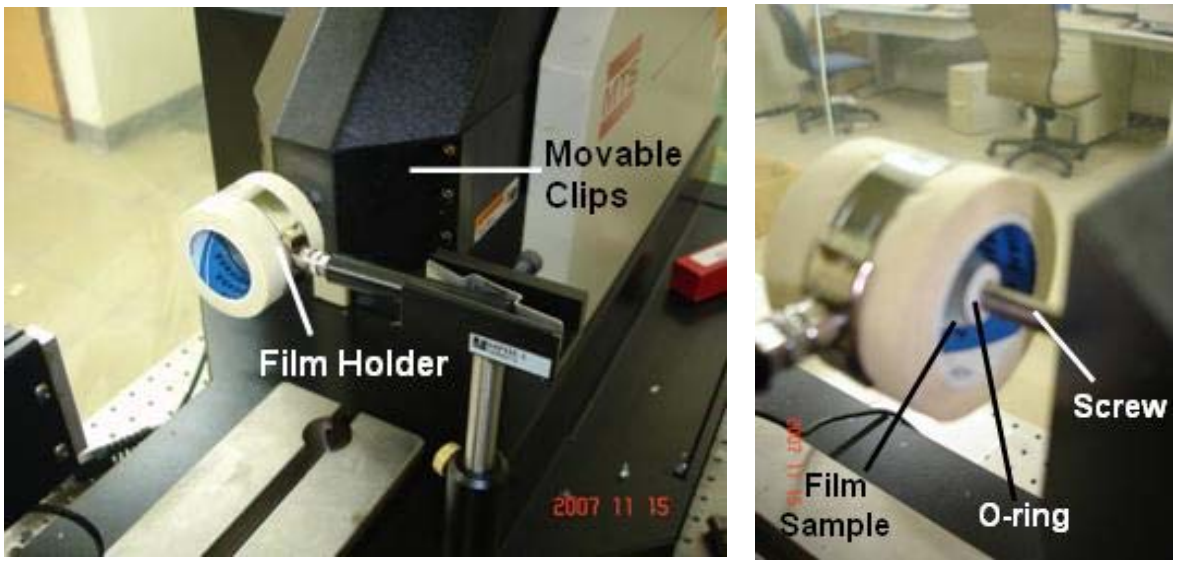

Figure 5.1 The pictures of the biaxial extension setup.

The formula of strain used here is as follow and the diagram is shown in figure 5.2:

$$\text{Strain} = (R'-R)/R*100\%$$

$$R' \fallingdotseq (R^2+L^2)^{1/2}$$

R: radius of the round sample

L: length stretched by tensile tester

According to the radius, we divided the round sample into three parts. The radius nearer to the circle of the round sample is 9mm and the farther one is 13mm (figure 5.2 (b)). On each radius we measured the transmittance of the film every ten degrees with a Helium-Neon (He-Ne). The diagram of optomechanical setup is shown in figure 5.3.

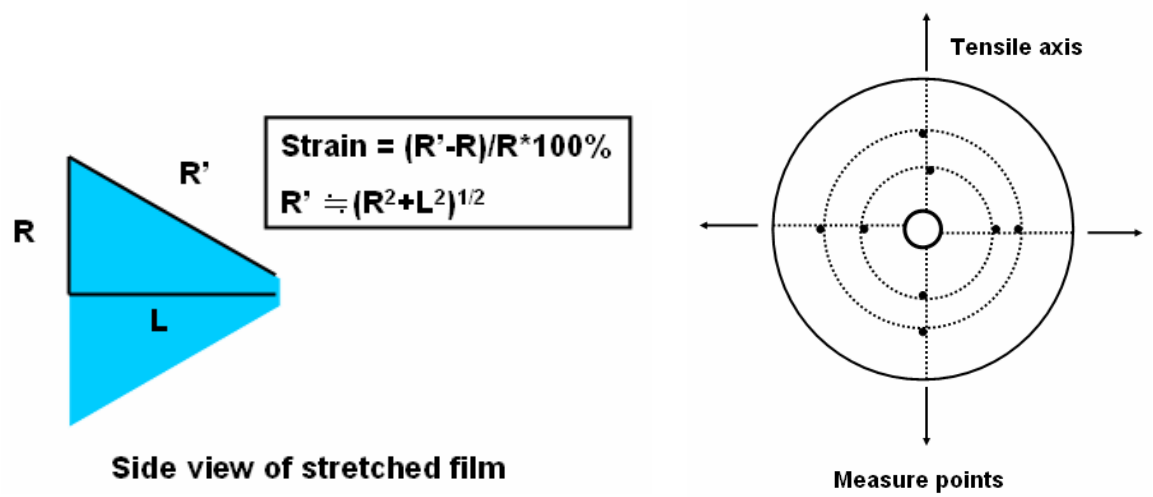

(a) (b)

Figure 5.2 (a):Side view of stretched film. (b): The three parts of the round sample.

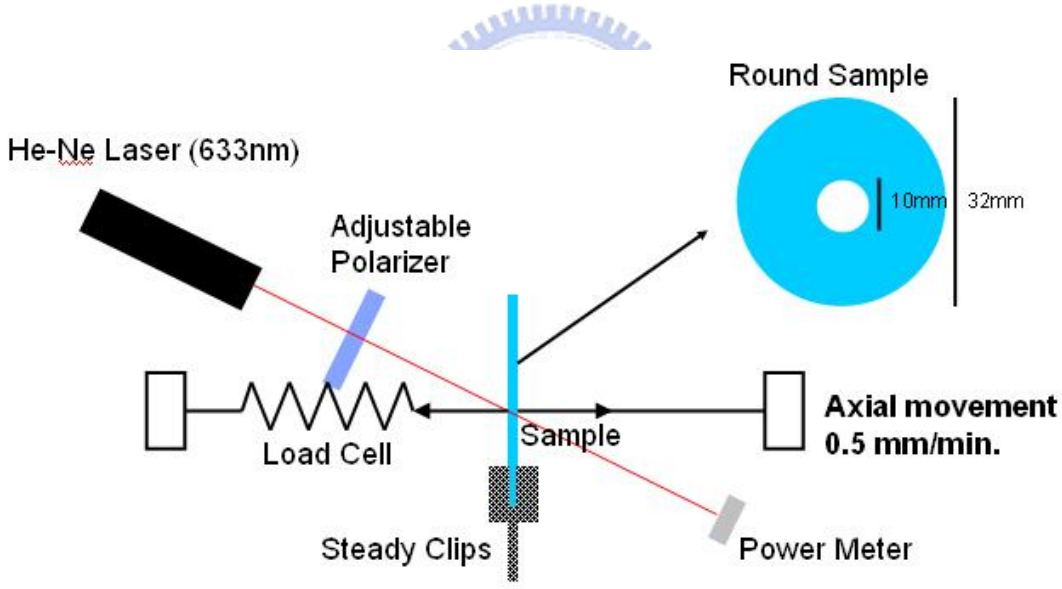

Figure 5.3 Schematic representation of optomechanical setup used for collecting measurements during applied strain.

First, we compared transmittance of PDLC films with different thickness, 10um and 20um when the strain was 100%. From the figure 5.4, we could see that the thinner the film was, the higher transmittance we could get and the transmittance

of the 10um film was almost 10 times to the 20um one. In this way, we took 10um as the parameter of thickness in this section.

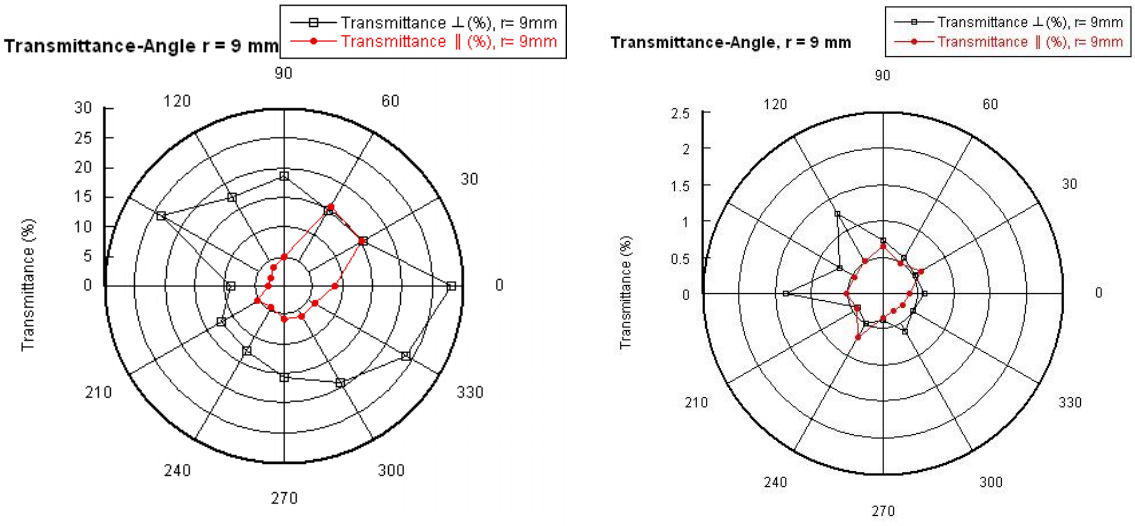

(a) (b)

Figure 5.4 Transmittance associated with different thickness of biaxial stretched PDLC films. The thickness of (a) is 10um and that of (b) is 20um

Sometimes we could see the diagrams of the transmittance and extinction ratio similar to the figure 5.5. The transmittance was much higher in one direction than others and the extinction ratio was much lower in that direction than others. It meant that PDLC film came off from the fixture. We should pay attention to this situation because it would affect the accuracy seriously.

We measured the transmittance of the film stretched along different radiuses, 9mm and 13mm shown in figure5.6. The transmittance was higher at radius 9mm than at 13mm. We tried different thickness from 10um to 20um and found that the tendency was more apparent when the films got thinker. In figure 5.6, the thickness of the film was 20um.

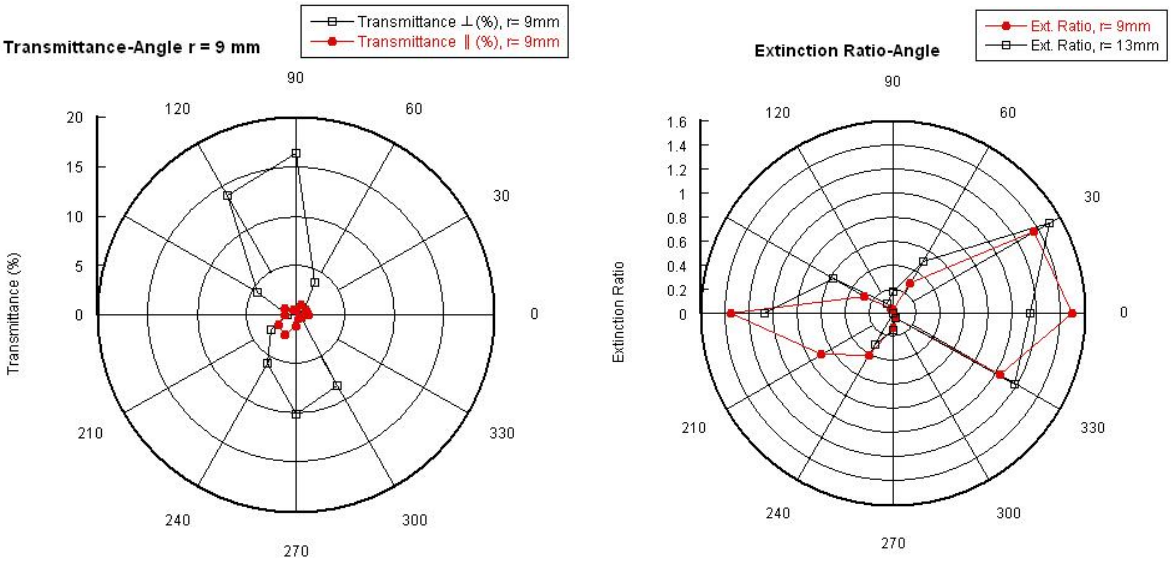

Figure 5.5 Transmittance and extinction ratio associated with different a biaxial stretched PDLC film which come off from the fixture.

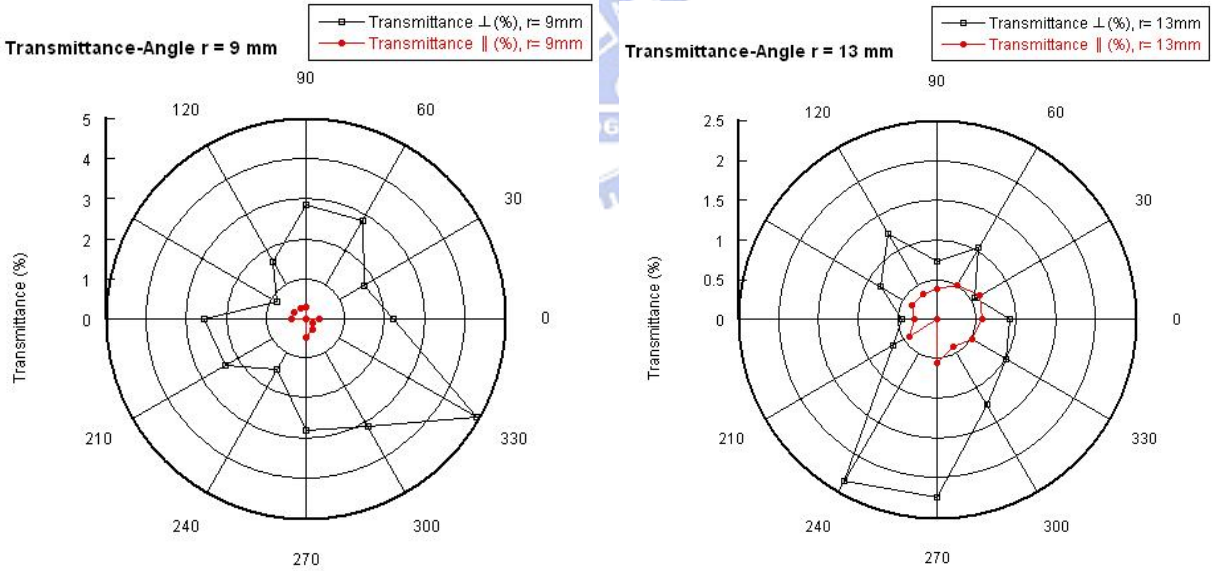

Figure 5.6 Transmittance associated with a biaxial stretch PDLC film at different radius. (a) is taken at r=9mm; (b) is taken at r=13mm.

After fixing the film properly and controlling the thickness of the film at 10um, the distribution of the extinction ratio becomes more uniform as shown in figure 5.7. It could be controlled under 0.5, and it was smaller at smaller radius. It

meant that we could get the characteristic of azimuthally polarized after stretching the PDLC film biaxially.

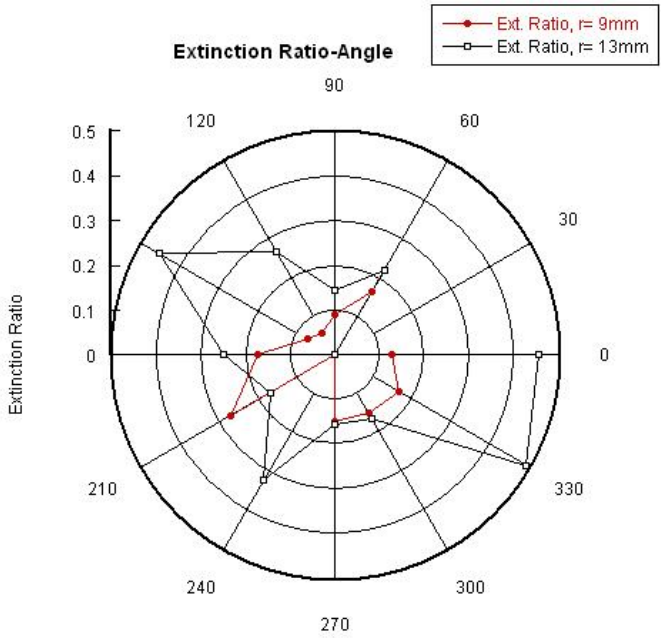

Figure 5.7 Extinction ratio associated with a biaxial stretched PDLC film measured from 0^{o} to 360^{o}

5.2 Polarizer Characteristic Experiment

As the concentration of E7 was 25wt%, the humidity was 50%, the thickness of the film was 10um, and it was cut in the shape of a round sample. We stretched the film biaxially till the strain was 100%. With a Helium-Neon (He-Ne) laser operating at 633 nm probing the sample at normal incidence, we controlled the polarization converter which can convert light into radial polarized light or azimuthal polarized light. Figures of photo shooting are shown in figure 5.8. In figure 5.8(a), the normal incidence is azimuthal polarized light. In figure 5.8(b), the normal incidence is radial polarized light. Comparing figure 5.8(a) and (b),

the biaxially stretched PDLC film presents like an azimuthal polarization converter. However, the film is not uniform enough so we still can see the radial polarized light cross the film form the figure 5.8(b).

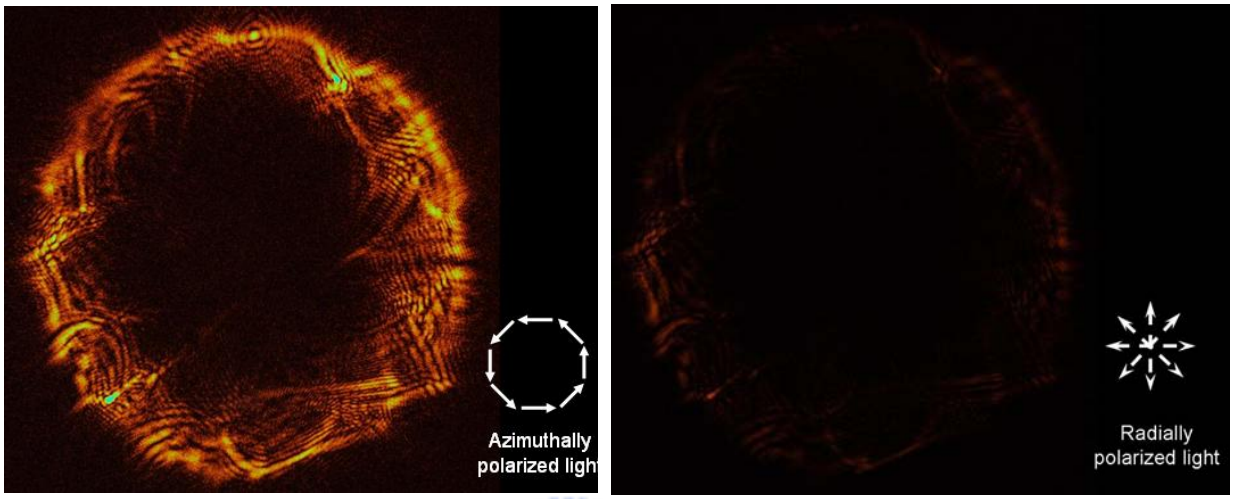

(a) (b)

Figure 5.8(a) The normal incidence is azimuthal polarized light; (b) the normal incidence is radial polarized light.

Chapter 6

Conclusions

6.1 Conclusions

We tried four ways, “R-to-R molding, spin coating, mold movement, and stretch” to get characteristic of linearly polarized. According to the experimental result, linearly polarized could be achieved by stretching. In addition, the experimental parameters have been analyzed and determined to achieve higher performance. The parameters of concentration, humidity, and thickness are shown in table 6.1:

Table 6.1 The parameters of concentration, humidity, and thickness

components	humidity	thickness of PDLC film
LC (E7): 25wt%	50%	10um

Basing on linearly polarized, we discussed about azimuthally polarized fatherly. We replaced uniaxial extension by biaxial extension, and determined some parameters during the experiment shown in table 6.2:

Table 6.2 The parameters of concentration, humidity, thickness, and strain

components	humidity	thickness of PDLC film	strain
LC (E7): 25wt%	50%	10um	100%

From the experimental results, we could see that no matter linearly or azimuthally polarized the highest transmittance was only 50%. In this way, surface scattering was still a key issue in this topic and measuring method should be improved.

6.2 Future Works

The stretched PDLC film really has a polarization selectivity. By utilizing these films for LCD applications scattered light might be recycled in a backlight system to ultimately improve the optical efficiency. This part should be take place in LCDs to know optical efficiency.

Biaxial extension of PDLC film for azimurhal polarizer could be achieved. However, the surface of the film is not uniform enough to be a azimuthal polarized converter. If there is a new way still applied biaxial extension is found to stretch the films uniformly, the azimuthal polarized converter will be fabricated inexpensively.

Reference

[1] F. Reinizer, Monatsh. Chem., **9**, 421 (1888).

[2] O. Lehmann, Z. Physik. Chem., **4**, 462 (1889).

[3] D. Demus, J. W. Goodby, G. W. Gray, H.-W. Spiess, and V. Vill, *Handbook of Liquid Crystals* (VCH, New York, 1998), Chap. 1.

[4] I. Amimori, J. N. Eakin, G. P. Crawford, N. V. Priezjev, and R. A. Pelcovits, SID DIGEST **24.3**, 834 (2002).

[5] I. Amimori, N. V. Priezjev, R. A. Pelcovits, and G. P. Crawford, Journal of Applied Physics, **93**, 6, 3248 (2003).

[6] J. N. Eakin, I. Amimori, and G. P. Crawford, *SPIE* ,San Diego, USA, August **2003, 5213**, 283.

[7] A. Nakajima, Gekkan Display, **6**, 38 (2000).

[8] O. A. Aphonin, YU. V. Panina, A. B. Pradin and D. A. Yakolev, Liquid Crystal, **15**, 395 (1993).

[9] J. W. Doane, D. K.Yang, and L. C. Chine, IDRC Technical Digest, 49 (1991).

[10] H. Ren, Y.-H. Lin, and S.-T. Wu, Applied Physics Letters, **89**, 051114 (2006)

[11] M. Stalder, and M. Schadt, Optics Letters, **21**, 23 (1996)

[12] P. S. Drzaic, *Liquid Crystal Dispersions* (World Scientific, Singapore, 1995), Chap. 2.

[13] H. Ren, Y. Lin, Y.-H. Fan, Y.-H. Fan, and S.-T. Wu, Applied Physics Letters, **86**, 141110 (2005).

[14] G. P. Montgomery, Jr., G. W. Smith, and N. A. Vaz, *Polymer-dispersed*

liquid crystal films (Springer-Verlag, New York, 1994), Chap. 2.

[15] J. W. Doane, *Polymer dispersed liquid crystal displays* (World Scientific, Singapore, 1990), Chap. 14.

[16] S. J. Klosowicz, M. Aleksander and P. Obrzut, Liquid Crystals, **5947**, 59470M-1 (2005).

[17] M. Aleksander, and S. J. Klosowicz, *SPIE*, San Diego, USA, August **2004, 5565**, 389.

[18] I. Amimori, J. N. Eakin, J. Qi, G. Skacej, S. Zumer, and G. P. Crawford, Physical Review E **71**, 031702 (2005).

[19] G. P. Montgomery, J. L. West, and W. Tamura-Lis, Journal of Applied Physics, 69, 1605 (1991).

[20] S. J. Klosowicz, and M. Aleksander, Opto-electronics Review, **12**, 305 (2004).

[21] R. M. Silverstein, G. C. Bassler, T.C. Morill, R.M. Silverstein, T. C. Morrill, *Spectrometric Identification of Organic Compounds* (John Wiley & Sons, Chichester 1991), 76-77.

[22] M. Pranga, K. L. Czuprynski and S. J. Klosowicz, *SPIE*, San Diego, USA, August 2000, 4147, 394.